Journal of Sound and Vibration (2002) **256**(4), 725–754
doi:10.1006/jsvi.5018, available online at http://www.idealibrary.com on IDEAL®

AN INVESTIGATION OF STABILITY IN THE LARGE BEHAVIOUR OF A CONTROL SURFACE WITH STRUCTURAL NON-LINEARITIES IN SUPERSONIC FLOW

A. P. Lewis

*Department of Aerospace, Civil and Mechanical Engineering, University of Hertfordshire, Hatfield, Hertfordshire AL*10 9*AB, England. E-mail: a.lewis@herts.ac.uk*

(*Received* 6 *September* 2001, *and in final form* 9 *January* 2002)

It is well known that the presence of non-linearities may significantly affect the aeroelastic response of an aerospace vehicle structure. In this paper, the aeroelastic behaviour at high Mach numbers of an all-moving control surface with a non-linearity in the root support is investigated. Very often, a stable equilibrium point, corresponding to zero displacement of the structure, together with an unstable limit cycle arising from a sub-critical Hopf bifurcation results from the presence of the non-linearity. The stable equilibrium point will then possess a domain of attraction. In this paper, this situation is investigated by first applying the averaging method to obtain a new set of aeroelastic equations in which the limit cycle is replaced by an unstable equilibrium point. A fourth order power series approximation to the stable manifold in the neighbourhood of this equilibrium point is then determined. From the stable manifold, predictions of the domain of attraction of the stable equilibrium point may then be made. The method is applied to two examples in which the non-linearity in the root support was due to either a cubic hardening restoring moment or the presence of freeplay. The approximation to the stable manifold was sufficient to enable significant information about the domain of attraction of the stable equilibrium point of the control surface to be obtained; agreement with predictions from numerical integration of the aeroelastic equations in the time domain was shown to be generally good in the cases considered, though outside the region of validity of the stable manifold expansion, discrepancies will occur. The averaging method was shown to be sufficiently accurate for this analysis even when the non-linearities could not be considered as weak.

1. INTRODUCTION

In carrying out aeroelastic analysis for an aircraft or missile, the structure, aerodynamics and controls (if considered) are generally modelled with the assumption of linearity. A major objective of the analysis is to determine a flutter boundary in terms of flight speed and various design parameters. In practice, non-linearities may be present that are capable of significantly affecting aeroelastic behaviour. Typical phenomena resulting from the presence of non-linearities include the onset of stable limit cycle oscillations through a super-critical Hopf bifurcation beyond the flutter boundary determined by linear theory, or the existence of unstable limit cycles within the linear flutter boundary associated with a sub-critical Hopf bifurcation. In the former case, the effect of the non-linearity may be regarded as beneficial if the limit cycle oscillations are small, whereas in the latter case, the non-linearities could lead to the possibility of divergent oscillations occurring within the

0022-460X/02/$30.00

linear flutter boundary as the equilibrium point of the system will possess some domain of attraction. It is this situation that is considered in this paper.

One approach to carrying out a theoretical study of non-linear aeroelastic behaviour is to perform the analysis in the time domain. However, a drawback with this is that though it can yield a complete picture of system behaviour for a particular set of initial conditions, it may be inefficient in providing an overall picture of system characteristics even for a single set of system parameters. In aeroelastic studies carried out during development of an aerospace vehicle, it is necessary to consider a wide range of flight conditions and design parameters, and thus there is a strong motivation to apply or develop alternative analysis techniques. Amongst these are averaging methods in which non-linearities are replaced by "equivalent" stiffnesses or dampings. These are attractive as they enable linear analysis techniques to be applied [1–9]. Perturbation methods have also been applied in the field of non-linear aeroelasticity; for example, Morino [10] performed a perturbation analysis of a non-linear panel flutter problem by means of the method of multiple time scales. A wide range of bifurcational behaviour may be encountered in non-linear aeroelastic systems, and a number of investigations have demonstrated this both theoretically and experimentally [11–16]. Consequently, the application of non-linear dynamical systems theory in the field of aeroelasticity is of great interest. Holmes [17] investigated panel flutter in terms of the bifurcations that are possible as in-plane load and air speed are varied, while Anderson [18] employed generic modelling to interpret observed non-linear transonic aeroelastic behaviour and to suggest the existence of new phenomena not previously encountered in computational studies. Smetlova and Dowell [13] studied the conditions necessary for chaotic motion of a buckled plate with external excitation in an aerodynamic flow. Centre manifold theory has been used to predict limit cycle oscillations in non-linear aeroelastic systems. Examples of this approach include Grzedzinski [19], Liu *et al.* [20] and Sedaghat *et al.* [21].

Many applications of the analysis techniques discussed above have been concerned with the investigation of possible limit cycles of non-linear aeroelastic systems. This paper considers an all-moving control surface flying under conditions where it possesses a stable equilibrium point O corresponding to zero structural displacement together with an unstable limit cycle, and is concerned with determining the resulting domain of attraction of O, and thus focuses on a slightly different aspect of the non-linear behaviour of aeroelastic systems. This is achieved through first applying the method of averaging to the aeroelastic equations. This reduces the number of degrees of freedom by one and also replaces the unstable limit cycle by a non-zero unstable equilibrium point in the averaged system of equations. The domain of attraction of the equilibrium point at O is then investigated through obtaining an approximation to the stable manifold of this unstable equilibrium point.

The use of the method of averaging in domain of stability estimation has been considered by Gilsinn [22], while the theoretical basis for the use of stable manifold analysis in the determination of a stability domain has been examined by Chiang *et al.* [23], who prove that for a fairly large class of autonomous non-linear systems, the stability boundary of a stable equilibrium point may be shown to consist of the stable manifolds of all equilibrium points and/or closed orbits on the stability boundary. The computation of the required stable manifolds is also discussed, though primarily for the case of planar systems. Venkatasubramanian and Ji [24] discuss numerical approximations to stable manifolds in large systems and show how the quadratic component of the stable manifold of an equilibrium point may be readily determined. In order to obtain a representation of the stability domain of the stable equilibrium point in a larger neighbourhood, higher terms are required. For the aeroelastic system considered in this paper, stable manifold computations

are carried out up to fourth order. The accuracy of this approximation to the stable manifold is then assessed by comparing the stability domain predictions it produces with results from integration of the aeroelastic equations in the time domain.

The layout of this paper is as follows. Section 2 briefly discusses the derivation of the aeroelastic equations for the all-moving control surface in high-speed supersonic flow. In section 3, the averaged form of the equations is obtained. Section 4 describes the approximation to the stable manifold of the unstable equilibrium point in the averaged set of equations corresponding to the unstable limit cycle of the original system, and also discusses the background to this approach to stability domain analysis. Section 5 presents results from this procedure and comparisons are made with predictions of the domain of attraction of the stable equilibrium point O obtained by numerical integration of the aeroelastic equations in their original form. Two examples of a non-linearity in the torsional degree of freedom of the root support of the control surface are considered; firstly, the case of a cubic hardening restoring moment is investigated, after which a freeplay non-linearity is analyzed. Concluding remarks are then given in section 6.

2. AEROELASTIC EQUATIONS

In this section, the form of the aeroelastic equations for an all-moving control surface with a single root support in a uniform supersonic flow is discussed. It is assumed that the control surface structure deforms linearly, and that the root support force-deflection characteristics are linear in bending but non-linear in torsion. The control surface is assumed to be performing small oscillations about a mean incidence angle of zero. The equations of motion for the control surface subjected to a set of external forces are first derived. These external forces comprise the aerodynamic loads obtained using third order piston theory [25] and the non-linear torsional moment about the control surface hinge line due to the root support.

The undisplaced control surface is illustrated in Figure 1. Fixed cartesian axes are defined with the origin P being the point where the root support is located. Control surface chordwise sections are assumed to be symmetrical, with the x-axis taken to be along the root chord line of symmetry with the positive direction towards the trailing edge; the y-axis is then the hinge line for the undeformed control surface, for which the x–y plane is a plane of symmetry. If the control surface is modelled as a plate structure, then its deformation may be defined in terms of vertical displacements of the mid-surface and rotations about the x- and y-axis. The control surface root chord is assumed to be unconstrained except at the root support P where bending and torsional rotations may occur, but no translational displacements are permitted. Modes and frequencies for the control surface are then determined for a given bending stiffness and an assumed linear torsional stiffness of the root support. Let the control surface modes be $\phi_1^F(x, y)$, $\phi_2^F(x, y)$, … and let the associated natural frequencies be $\omega_1^F, \omega_2^F, \ldots$. The generalized masses and stiffnesses of the control surface may then be evaluated and are denoted by $a_1^F, a_2^F, \ldots$ and $e_1^F, e_2^F, \ldots$ respectively.

Suppose now that the control surface is subject to external forces through aerodynamic loadings and torsional reaction loads due to the non-linearity in the root support. Then the equations of motion for the control surface may be obtained in the form

$$a_i^F \ddot{X}_i + \sum_j d_{ij}^F \dot{X}_j + e_i^F X_i = Q_{Mi} + Q_{Ai} \tag{1}$$

for $i = 1, 2, 3, \ldots$ where d_{ij}^F denotes a structural damping coefficient and $X_1, X_2, \ldots$ are generalized co-ordinates defining the control surface motion in terms of the modes $\phi_1^F(x, y)$,

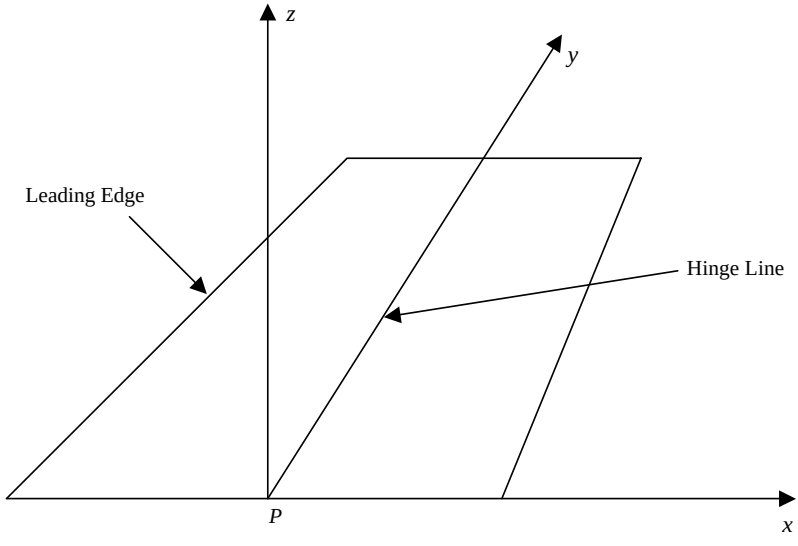

Figure 1. Lifting surface and axis system.

$\phi_2^F(x, y), \ldots$ Q_{Mi} is the ith generalized force due to the torsional reaction loads exerted on the control surface by the non-linearity in the root support and Q_{Ai} is the ith generalized force due to the aerodynamic loads.

Let M_y be the torsional moment acting on the control surface due to the non-linearity in the root support. Assuming that this is a non-linear function of the control surface root torsional angle θ_y and angular rate $\dot{\theta}_y$, Q_{Mi} is given by

$$Q_{Mi} = M_y(\theta_y, \dot{\theta}_y)\,\psi_{iy0}^F, \tag{2}$$

where ψ_{iy0}^F is the torsional rotation of the control surface at the root for the ith mode so that θ_y may be written:

$$\theta_y = \sum_i \psi_{iy0}^F X_i. \tag{3}$$

In this investigation, the aerodynamic loadings on the control surface are evaluated using third order piston theory [25] applied as strip theory so that the control surface is divided spanwise into a series of aerofoils undergoing heaving and pitching motions for which the lift and pitching moment may readily be determined. This approach is justifiable so long as the control surface does not have a very low aspect ratio or where significant chordwise deformations occur. Piston theory aerodynamics is applied at high supersonic speeds typically corresponding to Mach numbers between 2·5 and 7·0. The key assumption in piston theory is that the local pressure on an aerofoil surface is related to the normal component of the local fluid velocity in the same manner that the pressure on a piston in a fluid-filled tube is related to the velocity of the piston. In the form of the theory used for the present study, the pressure at a point on the fin surface is given by

$$p - p_\infty = \rho_\infty a_\infty^2 \left\{ \frac{w}{a_\infty} + \frac{1}{4}(\gamma + 1)\left(\frac{w}{a_\infty}\right)^2 + \frac{1}{12}(\gamma + 1)\left(\frac{w}{a_\infty}\right)^3 \right\}, \tag{4}$$

where w is the local downwash for the moving lifting surface, ρ_∞ is the free stream density, a_∞ the freestream speed of sound, p_∞ freestream pressure and γ the ratio of specific heats. In

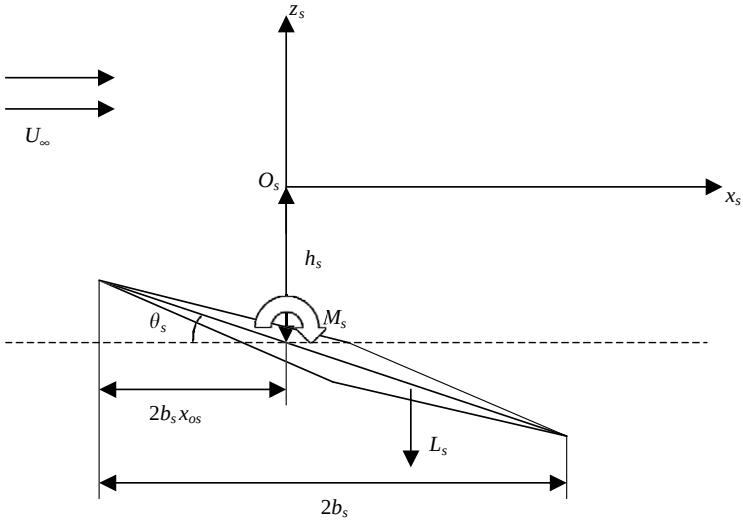

Figure 2. Notation for analysis of an aerofoil section.

general, the downwash may be written as a sum of steady state contributions due to thickness and mean angle of attack of the lifting surface together with unsteady contributions arising from its motion. In this study, a zero mean incidence is assumed, and only terms linear in unsteady displacements are retained.

Consider now the symmetric aerofoil section shown in Figure 2, having semi-chord b_s. In the undisturbed position, it lies with its line of symmetry along the $O_s x_s$-axis of a co-ordinate system where x_s, y_s, z_s are non-dimensionalized with respect to $2b_s$, with the leading edge a distance x_{os} forward of the origin O_s. The aerofoil thickness distribution, non-dimensionalized with respect to $2b_s$, is given by $\tau_s(x_s)$. The aerofoil lies in a uniform flow with velocity U_∞ and undergoes heaving and pitching motions h_s and θ_s as defined in Figure 2. Thus, the downwash on the aerofoil is given by

$$\frac{w}{U_\infty} = \pm\left[\frac{\dot{h}_s}{U_\infty} + \theta_s + \frac{2b_s}{U_\infty}(x_s - x_{0s})\,\dot{\theta}_s\right] + \frac{1}{2}\frac{\mathrm{d}\tau_s}{\mathrm{d}x_s}, \tag{5}$$

where the minus sign applies to the upper surface and the plus sign to the lower surface of the aerofoil. Substituting equation (5) into equation (4) will then enable the pressure difference between the upper and lower aerofoil surfaces to be obtained. The force per unit span L_s and the pitching moment M_s about O_s defined in the sense shown in Figure 2 may then be obtained. Given these, the aerodynamic loading on the lifting surface may now be determined by strip theory. Let the lifting surface be divided up into strips, capable of vertical translation and pitch rotation due to its elastic deformation as shown in Figure 3. h_s and θ_s are now the displacement and pitch rotation of the sth strip as shown. The average distance of the leading edge of the sth strip from the y_s-axis is $2b_s x_{os}$. Let b be the length of the root semi-chord. L_s and M_s are then given by

$$\begin{aligned} L_s &= -4\rho_\infty b U_\infty^2 \left\{\frac{\lambda_{s1}}{U_\infty M_\infty}\dot{h}_s + \frac{\lambda_{s2}}{M_\infty}\theta_s + \frac{\lambda_{s3}}{U_\infty M_\infty}\dot{\theta}_s\right\}, \\ M_s &= -4\rho_\infty b U_\infty^2 \left\{\frac{\mu_{s1}}{U_\infty M_\infty}\dot{h}_s + \frac{\mu_{s2}}{M_\infty}\theta_s + \frac{\mu_{s3}}{U_\infty M_\infty}\dot{\theta}_s\right\}, \end{aligned} \tag{6}$$

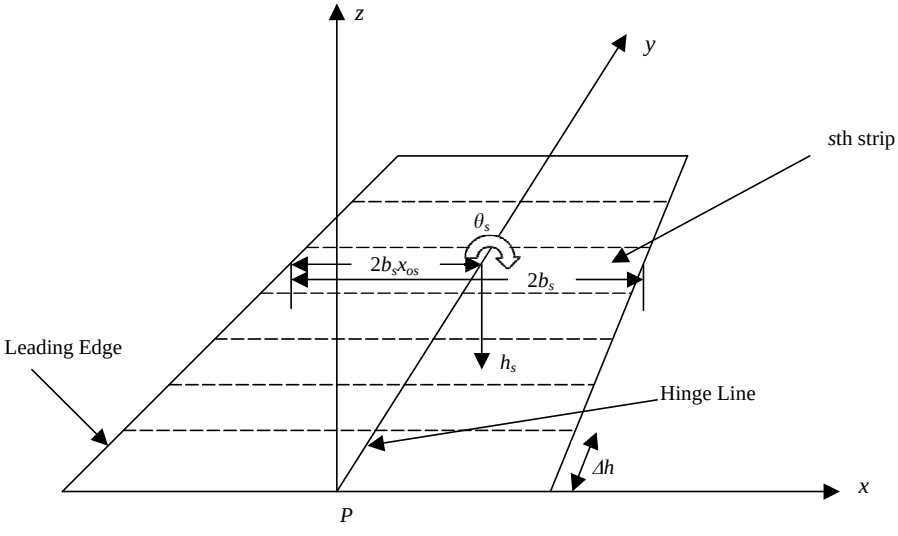

Figure 3. Notation used in implementation of strip theory.

where

$$\begin{aligned}
\lambda_{s1} &= \lambda_{s2} = \frac{b_s}{b}\left(1 + \frac{1}{4}(\gamma+1)M_\infty^2 I_{3s}\right),\\
\lambda_{s3} &= \frac{b_s^2}{b}\left\{1 - 2x_{os} + (\gamma+1)M_\infty I_{1s} + \frac{1}{2}(\gamma+1)M_\infty^2(I_{4s} - x_{os}I_{3s})\right\},\\
\mu_{s1} &= \mu_{s2} = \lambda_{s3},\\
\mu_{s3} &= \frac{b_s^3}{b}\left\{\frac{4}{3} - 4x_{os} + 4x_{os}^2 + 2(\gamma+1)(I_{2s} - 2x_{os}I_{1s})M_\infty\right.\\
&\quad \left. + (\gamma+1)M_\infty^2(I_{5s} - 2x_{os}I_{4s} + x_{os}^2 I_{3s})\right\}
\end{aligned} \tag{7}$$

and I_{1s}, I_{2s}, I_{3s}, I_{4s} and I_{5s} are functions of thickness distribution and are given by

$$\begin{aligned}
&I_{1s} = \frac{1}{2}\int_0^1 x_s \frac{d\tau_s}{dx_s}\,dx_s, \quad I_{2s} = \frac{1}{2}\int_0^1 x_s^2 \frac{d\tau_s}{dx_s}\,dx_s, \quad I_{3s} = \frac{1}{4}\int_0^1 \left(\frac{d\tau_s}{dx_s}\right)^2 dx_s,\\
&I_{4s} = \frac{1}{4}\int_0^1 x_s\left(\frac{d\tau_s}{dx_s}\right)^2 dx_s, \quad I_{5s} = \frac{1}{4}\int_0^1 x_s^2\left(\frac{d\tau_s}{dx_s}\right)^2 dx_s,
\end{aligned} \tag{8}$$

where it is assumed that the leading and trailing edge thicknesses are zero so that $\tau_s(0) = \tau_s(1) = 0$. Denote by ϕ_{is}^F and ψ_{iys}^F the ith modal displacement and rotation of the sth strip. Then h_s and θ_s may be written in terms of generalized displacements as

$$\begin{aligned}
h_s &= -\sum_i \phi_{is}^F X_i,\\
\theta_s &= \sum_i \psi_{iys}^F X_i.
\end{aligned} \tag{9}$$

The virtual work per unit span on the sth strip by the aerodynamic forces in producing a translation δh_s and pitch rotation $\delta\theta_s$ as a result of increments δX_1, δX_2, ... in the

generalized displacements may then be determined, from which the generalized aerodynamic force for the sth strip, Q^A_{si}, can be found from

$$Q^A_{si} = \Delta h(M_s \psi^F_{iys} - L_s \phi^F_{is}), \tag{10}$$

where Δh is the strip width. Making use of equations (6)–(9) in equation (10) then leads to the following expression for Q^A_{si}:

$$Q^A_{si} = -4\rho_\infty U^2_\infty b \Delta h \sum_j \left[\frac{A^s_{ij}}{M_\infty} X_j + \frac{B^s_{ij}}{M_\infty U_\infty} \dot{X}_j \right], \tag{11}$$

where A^s_{ij} and B^s_{ij} are given by

$$\begin{aligned} A^s_{ij} &= \mu_{s2} \psi^F_{iys} \psi^F_{jys} - \lambda_{s2} \phi^F_{is} \psi^F_{jys}, \\ B^s_{ij} &= -\mu_{s3} \psi^F_{iys} \psi^F_{jys} - \mu_{s1} \phi^F_{js} \psi^F_{iys} + \lambda_{s1} \phi^F_{is} \phi^F_{js} + \lambda_{s3} \psi^F_{jys} \phi^F_{is}. \end{aligned} \tag{12}$$

The ith generalized force for the overall aerodynamic loading on the lifting surface is then obtained by summing the contributions for all strips. Thus writing

$$R_{ij} = \Delta h \sum_s A^s_{ij}, \quad I_{ij} = \Delta h \sum_s B^s_{ij} \tag{13}$$

enables the generalized force Q_{Ai} due to the aerodynamic forces to be written in terms of the generalized displacements $X_1, X_2, X_3, \ldots$ in the following way:

$$Q_{Ai} = -4\rho_\infty U^2_\infty b \sum_j \left[\frac{R_{ij}}{M_\infty} X_j + \frac{I_{ij}}{M_\infty U_\infty} \dot{X}_j \right]. \tag{14}$$

Combining equations (1), (2) and (14) then yields the aeroelastic equations in the form:

$$\ddot{\mathbf{X}} + \mathbf{G}\dot{\mathbf{X}} + \mathbf{H}\mathbf{X} + \varepsilon f(\mathbf{r}^{\mathrm{T}}\mathbf{X}, \mathbf{r}^{\mathrm{T}}\dot{\mathbf{X}})\mathbf{s} = \mathbf{0}, \tag{15}$$

where $\mathbf{X}$ is the column vector of the generalized co-ordinates $X_1, X_2, \ldots, \varepsilon$ is a parameter governing the strength of the non-linearity. $\mathbf{G}$ and $\mathbf{H}$ are damping and stiffness matrices whose elements are given by

$$\begin{aligned} G_{ij} &= \frac{d^F_{ij}}{a^F_i} \delta_{ij} + \frac{4\rho_\infty b U^2_\infty I_{ij}}{M_\infty U_\infty a^F_i}, \\ H_{ij} &= \frac{e^F_i}{a^F_i} \delta_{ij} + \frac{4\rho_\infty b U^2_\infty R_{ij}}{M_\infty a^F_i} \end{aligned} \tag{16}$$

and $\mathbf{r}$, $\mathbf{s}$ are column vectors whose elements are given by

$$r_i = \psi^F_{iy0}, \quad s_i = \frac{\psi^F_{iy0}}{a^F_i} \tag{17}$$

so that

$$\theta_y = \mathbf{r}^{\mathrm{T}}\mathbf{X}; \qquad \varepsilon f(\mathbf{r}^{\mathrm{T}}\mathbf{X}, \mathbf{r}^{\mathrm{T}}\dot{\mathbf{X}}) = -M_y(\theta_y, \dot{\theta}_y). \tag{18}$$

These aeroelastic equations will be solved numerically in the time domain and also using the averaging method as described in section 3.

3. APPLICATION OF THE METHOD OF AVERAGING

In this section, the application of the method of averaging to the analysis of equation (15) is described. It will now be assumed that the motion of the control surface is described by

the lowest two modes of the structure only, so that the aeroelastic equations become a two-degree-of-freedom second order system. In the linear case, the flutter behaviour of a lifting surface alone may frequently be determined with acceptable accuracy by an analysis involving only these modes, particularly in the case where one mode involves predominantly bending and the other involves mostly torsion. In this investigation, the form of the aeroelastic equations used in the non-linear analysis has therefore been kept as simple as possible, with the potential effect of higher modes on the stability domain analysis lying outside the scope of this study. Equation (15) may now be written as a four-degree-of-freedom first order system as follows:

$$\bar{\mathbf{U}}\begin{pmatrix}\dot{\mathbf{X}}\\ \dot{\mathbf{Y}}\end{pmatrix} = \bar{\mathbf{V}}\begin{pmatrix}\mathbf{X}\\ \mathbf{Y}\end{pmatrix} - \varepsilon\begin{pmatrix}\mathbf{0}\\ \mathbf{s}\end{pmatrix} f, \tag{19}$$

where

$$\bar{\mathbf{U}} = \begin{pmatrix} -\mathbf{H} & \mathbf{0}\\ \mathbf{0} & \mathbf{I}\end{pmatrix}, \qquad \bar{\mathbf{V}} = \begin{pmatrix} \mathbf{0} & -\mathbf{H}\\ -\mathbf{H} & \mathbf{G}\end{pmatrix}. \tag{20}$$

$\mathbf{I}$ denotes the (2×2) identity matrix and $\mathbf{Y} = \dot{\mathbf{X}}$. Let $\bar{\mathbf{N}}$ and $\bar{\mathbf{M}}$ denote the left- and right-hand modal matrices that would arise in the eigenvalue problem that would occur when solving equation (19) for $f = 0$. These will then have the form

$$\bar{\mathbf{M}} = \begin{bmatrix}\mathbf{M} & \mathbf{M}^*\\ \mathbf{M}\boldsymbol{\mu} & \mathbf{M}^*\boldsymbol{\mu}^*\end{bmatrix}; \qquad \bar{\mathbf{N}} = \begin{bmatrix}\mathbf{N} & \boldsymbol{\mu}\mathbf{N}\\ \mathbf{N}^* & \mathbf{N}^*\boldsymbol{\mu}^*\end{bmatrix}, \tag{21}$$

where $\boldsymbol{\mu} = \text{diag}\{\mu_1, \mu_2\}$ with μ_1, μ_2 being the eigenvalues and * denoting the complex conjugate. In this study, it is assumed that in the linearized aeroelastic equations considered μ_1, μ_2 will always possess both non-zero real and imaginary parts. Now define co-ordinates Q_1, Q_2, Q_3, Q_4 by the linear transformation

$$\begin{pmatrix}\mathbf{X}\\ \mathbf{Y}\end{pmatrix} = \begin{bmatrix}\text{Re}(\mathbf{M}) - \text{Im}(\mathbf{M}) & \text{Re}(\mathbf{M}) + \text{Im}(\mathbf{M})\\ \text{Re}(\mathbf{M}\boldsymbol{\mu}) - \text{Im}(\mathbf{M}\boldsymbol{\mu}) & \text{Re}(\mathbf{M}\boldsymbol{\mu}) + \text{Im}(\mathbf{M}\boldsymbol{\mu})\end{bmatrix}\begin{pmatrix}Q_1\\ Q_2\\ Q_3\\ Q_4\end{pmatrix}. \tag{22}$$

With this transformation, equations (19) may now be written:

$$\begin{pmatrix}\dot{Q}_1\\ \dot{Q}_2\\ \dot{Q}_3\\ \dot{Q}_4\end{pmatrix} = \begin{pmatrix}\lambda_1 & 0 & \omega_1 & 0\\ 0 & \lambda_2 & 0 & \omega_2\\ -\omega_1 & 0 & \lambda_1 & 0\\ 0 & -\omega_2 & 0 & \lambda_2\end{pmatrix}\begin{pmatrix}Q_1\\ Q_2\\ Q_3\\ Q_4\end{pmatrix} - \varepsilon\begin{pmatrix}\text{Re}(\sigma_1) + \text{Im}(\sigma_1)\\ \text{Re}(\sigma_2) + \text{Im}(\sigma_2)\\ \text{Re}(\sigma_1) - \text{Im}(\sigma_1)\\ \text{Re}(\sigma_2) - \text{Im}(\sigma_2)\end{pmatrix} f, \tag{23}$$

where σ_1, σ_2 are defined by $(\sigma_1, \sigma_2)^{\text{T}} = \boldsymbol{\sigma} = \boldsymbol{\mu}\mathbf{N}\mathbf{s}$ and $\mu_k = \lambda_k + \text{i}\omega_k$. It should be noted that ω_1 and ω_2 are the frequencies of the aeroelastic modes and are distinct from the lifting surface structure natural frequencies ω_1^F and ω_2^F. The method of averaging assumes that the non-linearities in the system result in an oscillatory solution with slowly varying amplitude and phase. Let the displacements Q_1, Q_2, Q_3, Q_4 now be transformed into a new set of

displacements a_1, a_2, a_3, a_4 by

$$\begin{pmatrix} Q_1 \\ Q_2 \\ Q_3 \\ Q_4 \end{pmatrix} = \begin{bmatrix} \sin\omega_1 t & 0 & \cos\omega_1 t & 0 \\ 0 & \sin\omega_2 t & 0 & \cos\omega_2 t \\ \cos\omega_1 t & 0 & -\sin\omega_1 t & 0 \\ 0 & \cos\omega_2 t & 0 & -\sin\omega_2 t \end{bmatrix} \begin{pmatrix} a_1 \\ a_2 \\ a_3 \\ a_4 \end{pmatrix}, \tag{24}$$

where a_1, a_2, a_3, a_4 will be assumed to be slowly varying. In terms of these new displacements, equations (23) may now be written:

$$\begin{pmatrix} \dot{a}_1 \\ \dot{a}_2 \\ \dot{a}_3 \\ \dot{a}_4 \end{pmatrix} = \begin{pmatrix} \lambda_1 a_1 \\ \lambda_2 a_2 \\ \lambda_1 a_3 \\ \lambda_2 a_4 \end{pmatrix} - \varepsilon \begin{bmatrix} \sin\omega_1 t & 0 & \cos\omega_1 t & 0 \\ 0 & \sin\omega_2 t & 0 & \cos\omega_2 t \\ \cos\omega_1 t & 0 & -\sin\omega_1 t & 0 \\ 0 & \cos\omega_2 t & 0 & -\sin\omega_2 t \end{bmatrix} \begin{pmatrix} \sigma_{1R} + \sigma_{1I} \\ \sigma_{2R} + \sigma_{2I} \\ \sigma_{1R} - \sigma_{1I} \\ \sigma_{2R} - \sigma_{2I} \end{pmatrix} f, \tag{25}$$

where $\sigma_{iR} = \mathrm{Re}(\sigma_i)$, $\sigma_{iI} = \mathrm{Im}(\sigma_i)$. Let the following transformation now be applied:

$$a_1 = A_1 \cos\phi_1, \quad a_2 = A_2 \cos\phi_2, \quad a_3 = A_1 \sin\phi_1, \quad a_4 = A_2 \sin\phi_2. \tag{26}$$

Equations (25) may now be transformed into the following form:

$$\begin{pmatrix} \dot{A}_1 - \lambda_1 A_1 \\ \dot{A}_2 - \lambda_2 A_2 \\ A_1\dot{\phi}_1 \\ A_2\dot{\phi}_2 \end{pmatrix} = -\varepsilon\sqrt{2} \begin{pmatrix} \sigma_{1R}\sin(\omega_1 t + \phi_1 + \pi/4) - \sigma_{1I}\cos(\omega_1 t + \phi_1 + \pi/4) \\ \sigma_{2R}\sin(\omega_2 t + \phi_2 + \pi/4) - \sigma_{2I}\cos(\omega_2 t + \phi_2 + \pi/4) \\ \sigma_{1R}\cos(\omega_1 t + \phi_1 + \pi/4) + \sigma_{1I}\sin(\omega_1 t + \phi_1 + \pi/4) \\ \sigma_{2R}\cos(\omega_2 t + \phi_2 + \pi/4) + \sigma_{2I}\sin(\omega_2 t + \phi_2 + \pi/4) \end{pmatrix} f. \tag{27}$$

The arguments of the function f are $\mathbf{r}^{\mathrm{T}}\mathbf{X}$ and $\mathbf{r}^{\mathrm{T}}\dot{\mathbf{X}}$. In terms of the variables A_1, A_2, ϕ_1, ϕ_2, $\mathbf{r}^{\mathrm{T}}\mathbf{X}$ may be written:

$$\begin{aligned} \mathbf{r}^{\mathrm{T}}\mathbf{X} = \sqrt{2}\{&A_1\mathbf{r}^{\mathrm{T}}\,\mathrm{Re}(\mathbf{M}_1)\sin(\omega_1 t + \phi_1 + \pi/4) + A_1\mathbf{r}^{\mathrm{T}}\,\mathrm{Im}(\mathbf{M}_1)\cos(\omega_1 t + \phi_1 + \pi/4) \\ &+ A_2\mathbf{r}^{\mathrm{T}}\,\mathrm{Re}(\mathbf{M}_2)\sin(\omega_2 t + \phi_2 + \pi/4) + A_2\mathbf{r}^{\mathrm{T}}\mathrm{Im}(\mathbf{M}_2)\cos(\omega_2 t + \phi_2 + \pi/4)\}, \end{aligned} \tag{28}$$

where $\mathbf{M}_i$ denotes the ith column of $\mathbf{M}$. Now define $\psi_1 = \omega_1 t + \phi_1 + \pi/4$ and $\psi_2 = \omega_2 t + \phi_2 + \pi/4$. Then the final form of the transformed equations is

$$\begin{pmatrix} \dot{A}_1 - \lambda_1 A_1 \\ \dot{A}_2 - \lambda_2 A_2 \\ A_1(\dot{\psi}_1 - \omega_1) \\ A_2(\dot{\psi}_2 - \omega_2) \end{pmatrix} = -\varepsilon\sqrt{2} \begin{pmatrix} \sigma_{1R}\sin\psi_1 - \sigma_{1I}\cos\psi_1 \\ \sigma_{2R}\sin\psi_2 - \sigma_{2I}\cos\psi_2 \\ \sigma_{1R}\cos\psi_1 + \sigma_{1I}\sin\psi_1 \\ \sigma_{2R}\cos\psi_2 + \sigma_{2I}\sin\psi_2 \end{pmatrix} f \tag{29}$$

and

$$\begin{aligned} \mathbf{r}^{\mathrm{T}}\mathbf{X} = \sqrt{2}\{&A_1\mathbf{r}^{\mathrm{T}}\,\mathrm{Re}(\mathbf{M_1})\sin\psi_1 + A_1\mathbf{r}^{\mathrm{T}}\,\mathrm{Im}(\mathbf{M}_1)\cos\psi_1 \\ &+ A_2\mathbf{r}^{\mathrm{T}}\,\mathrm{Re}(\mathbf{M}_2)\sin\psi_2 + A_2\mathbf{r}^{\mathrm{T}}\,\mathrm{Im}(\mathbf{M}_2)\cos\psi_2\}. \end{aligned} \tag{30}$$

The right-hand side of equation (29) may now in principle be expanded to give a term independent of ψ_1 and ψ_2 which will be slowly varying together with terms containing $\cos(n\psi_1 \pm m\psi_2)$ and $\sin(n\psi_1 \pm m\psi_2)$. For the aeroelastic problem considered, it will be the case that $\omega_1 - \omega_2$ is small, and hence can be taken to be $\mathrm{O}(\varepsilon)$, so that it is possible to write

$\psi_2 = \psi_1 + \theta$ where now θ will be slowly varying. This is because the non-linear behaviour studied is closely associated with flutter of the linear system, and the onset of flutter is linked with the phenomenon of frequency coalescence. In addition, the aerodynamic damping will be light so that λ_1 and λ_2 will turn out to be small. Taking these factors into account, averaging is now carried out with respect to the remaining fast varying variable ψ_1 by integrating equations (29) with respect to ψ_1 from 0 to 2π to give

$$\dot{A}_1 = \lambda_1 A_1 - \frac{\varepsilon\sqrt{2}}{2\pi}\int_0^{2\pi}(\sigma_{1R}\sin\psi_1 - \sigma_{1I}\cos\psi_1) f\,\mathrm{d}\psi_1,$$

$$\dot{A}_2 = \lambda_2 A_2 - \frac{\varepsilon\sqrt{2}}{2\pi}\int_0^{2\pi}(\sigma_{2R}\sin(\theta+\psi_1) - \sigma_{2I}\cos(\theta+\psi_1)) f\,\mathrm{d}\psi_1,$$

$$\dot{\theta} = \omega_2 - \omega_1 - \frac{\varepsilon\sqrt{2}}{2\pi A_2}\int_0^{2\pi}(\sigma_{2R}\cos(\theta+\psi_1) + \sigma_{2I}\sin(\theta+\psi_1)) f\,\mathrm{d}\psi_1$$
$$+ \frac{\varepsilon\sqrt{2}}{2\pi A_1}\int_0^{2\pi}(\sigma_{1R}\cos\psi_1 + \sigma_{1I}\sin\psi_1) f\,\mathrm{d}\psi_1. \tag{31}$$

Equations (15) and (29) have now been reduced to a three-degree-of-freedom system in the variables A_1, A_2 and θ. The equilibrium point $Q_1 = Q_2 = Q_3 = Q_4 = 0$ in equations (19) will become $A_1 = A_2 = 0$, $\theta = (\omega_2 - \omega_1)t + \theta_0$ in equations (31). A limit cycle in equations (15) and (19) will become an equilibrium point $(A_1^0,\ A_2^0,\ \theta^0)$ in equations (31).

4. DETERMINATION OF THE STABLE MANIFOLD

The problem analyzed in this study is that of estimating the domain of attraction of the zero-displacement stable equilibrium point of the control surface that typically arises following a sub-critical Hopf bifurcation. Let this equilibrium point be denoted by O. The method of averaging has been applied to the aeroelastic equations to produce a three-degree-of-freedom system in which the unstable limit cycle corresponds to an unstable equilibrium point. It may then be anticipated that the stable manifold of this fixed point $(A_1^0,\ A_2^0,\ \theta^0)$ in the averaged system will approximate the stable manifold of the unstable limit cycle in the aeroelastic equations. The approach to predicting the domain of attraction of the stable equilibrium point O makes use of the work of Chiang *et al.* [23]. They showed that under certain conditions, the stability boundary of O is composed of the stable manifolds of all the critical elements (equilibrium points or closed orbits) on the stability boundary. These conditions are: (1) all the critical elements on the stability boundary are hyperbolic—a generic property of continuous dynamic systems; (2) the stable and unstable manifolds of critical elements on the stability boundary satisfy the transversality condition—again a generic property though not easy to check [23]; (3) every trajectory on the stability boundary approaches one of the critical elements as $t \to \infty$. Assumption (3) is not a generic property [23]. For the case of systems with only equilibrium points on the stability boundary, the third assumption may be verified by use of a number of results based on the introduction of a function resembling a Lyapunov function. Identifying a suitable function for high order systems may not be easy; furthermore, for systems with closed orbits on the stability boundary, the situation appears to be even more difficult. However, even if Assumption (3) is not presumed to hold, it may be shown that if the intersection of the stability domain of O and its closure with the unstable manifold of an unstable equilibrium point or closed orbit is non-empty, then that unstable equilibrium

point or closed orbit lies on the boundary of the domain of attraction. This condition may be readily checked numerically. Furthermore, the intersection of the stable manifold of the unstable equilibrium point or closed orbit and the boundary of the domain of attraction of O will be non-empty. The stability boundary of O for the aeroelastic system will be investigated by determining the stable manifold of the unstable equilibrium point in the averaged system by a power series expansion; thus, the stable manifold will be determined in a neighbourhood of the equilibrium point only. In the light of the above discussion, this approach seems reasonable even if Assumption (3) cannot be readily shown to apply to the system. The expansion was taken up to fourth order, which was found to be sufficient for studying the domains of attraction of the aeroelastic systems considered, as will be shown in section 5.

Stable manifold analysis is now carried out for the fixed point $(A_1^0,\ A_2^0,\ \theta^0)$ of the averaged system of equations (31). To do this, equations (31) are first written as

$$\begin{pmatrix} \dot{A}_1 \\ \dot{A}_2 \\ \dot{\theta} \end{pmatrix} = \mathbf{A} \begin{pmatrix} A_1 - A_1^0 \\ A_2 - A_2^0 \\ \theta - \theta^0 \end{pmatrix} + \mathbf{R}(A_1 - A_1^0, A_2 - A_2^0, \theta - \theta^0), \tag{32}$$

where $\mathbf{A}$ denotes the Jacobian matrix of the right-hand side of equations (31) and the vector $\mathbf{R}$ consists of the non-linear terms of the system. A linear transformation $\mathbf{Q}$ based on the eigenvectors of $\mathbf{A}$ is now defined which uncouples the dynamics of equations (32) in a linear sense as follows:

$$\begin{pmatrix} A_1 - A_1^0 \\ A_2 - A_2^0 \\ \theta - \theta^0 \end{pmatrix} = \mathbf{Q} \begin{pmatrix} u_1 \\ u_2 \\ v \end{pmatrix} \tag{33}$$

and

$$\mathbf{Q}^{-1}\mathbf{A}\mathbf{Q} = \begin{pmatrix} \mathbf{A}_s & \mathbf{0} \\ \mathbf{0} & \lambda_u \end{pmatrix}, \tag{34}$$

where λ_u is the positive real eigenvalue of $\mathbf{A}$ and $\mathbf{A}_s$ is a (2×2) matrix whose eigenvalues have negative real parts. In the case where the eigenvalues of $\mathbf{A}_s$ are real, the columns of $\mathbf{Q}$ will consist of the eigenvectors of the Jacobian matrix $\mathbf{A}$ and $\mathbf{A}_s$ will be diagonal. In terms of the variables u_1, u_2, v, equations (32) may now be written:

$$\begin{pmatrix} \dot{u}_1 \\ \dot{u}_2 \\ \dot{v} \end{pmatrix} = \begin{pmatrix} \mathbf{A}_s & \mathbf{0} \\ \mathbf{0} & \lambda_u \end{pmatrix} \begin{pmatrix} u_1 \\ u_2 \\ v \end{pmatrix} + \mathbf{Q}^{-1}\mathbf{R}\left\{ \mathbf{Q} \begin{pmatrix} u_1 \\ u_2 \\ v \end{pmatrix} \right\}. \tag{35}$$

Thus, equations (32) may now be decoupled in the linear sense and written as

$$\begin{pmatrix} \dot{u}_1 \\ \dot{u}_2 \end{pmatrix} = \mathbf{A}_s \begin{pmatrix} u_1 \\ u_2 \end{pmatrix} + \mathbf{R}_s(u_1, u_2, v),$$

$$\dot{v} = \lambda_u v + R_u(u_1,\ u_2,\ v), \tag{36}$$

where $\mathbf{R}_s$ and R_u consist of the non-linear terms of the system. Let the stable manifold of the equilibrium point $(A_1^0,\ A_2^0,\ \theta^0)$, or equivalently $u_1 = u_2 = v = 0$, be expressed as

$v = h(u_1, u_2)$. Then h must satisfy the partial differential equation

$$\lambda_u h(u_1, u_2) + R_u(u_1, u_2, h(u_1, u_2)) = \left(\frac{\partial h}{\partial u_1}\ \frac{\partial h}{\partial u_2}\right)\left\{\mathbf{A}_s\begin{pmatrix}u_1\\u_2\end{pmatrix} + \mathbf{R}_s(u_1, u_2, h(u_1, u_2))\right\}, \quad (37)$$

where $h(0,0) = \partial h(0,0)/\partial u_1 = \partial h(0,0)/\partial u_2 = 0$. Now define $h(u_1, u_2) = h_2(u_1, u_2) + h_3(u_1, u_2) + h_4(u_1, u_2) + \cdots$ where h_n contains all the nth order terms of h. Substituting this form for h in equation (37) and equating second, third and fourth order terms gives:

$$\lambda_u h_2(u_1, u_2) + O_2(R_u(u_1, u_2, 0)) = \left(\frac{\partial h_2}{\partial u_1}\ \frac{\partial h_2}{\partial u_2}\right)\mathbf{A}_s\begin{pmatrix}u_1\\u_2\end{pmatrix}, \quad (38)$$

$$\lambda_u h_3(u_1, u_2) + O_3(R_u(u_1, u_2, h_2)) = \left(\frac{\partial h_3}{\partial u_1}\ \frac{\partial h_3}{\partial u_2}\right)\mathbf{A}_s\begin{pmatrix}u_1\\u_2\end{pmatrix} + \left(\frac{\partial h_2}{\partial u_1}\ \frac{\partial h_2}{\partial u_2}\right)O_2(\mathbf{R}_s(u_1, u_2, 0)), \quad (39)$$

$$\begin{aligned}\lambda_u h_4(u_1, u_2) + O_4(R_u(u_1, u_2, h_2 + h_3)) = {} & \left(\frac{\partial h_4}{\partial u_1}\ \frac{\partial h_4}{\partial u_2}\right)\mathbf{A}_s\begin{pmatrix}u_1\\u_2\end{pmatrix} \\ & + \left(\frac{\partial h_3}{\partial u_1}\ \frac{\partial h_3}{\partial u_2}\right)O_2(\mathbf{R}_s(u_1, u_2, 0)) \\ & + \left(\frac{\partial h_2}{\partial u_1}\ \frac{\partial h_2}{\partial u_2}\right)O_3(\mathbf{R}_s(u_1, u_2, h_2)) \end{aligned} \quad (40)$$

with similar equations for higher order terms. Using equation (38), h_2 may be readily obtained by first writing

$$h_2 = (u_1\ u_2)\,\mathbf{H}_2\begin{pmatrix}u_1\\u_2\end{pmatrix}, \quad (41)$$

where $\mathbf{H}_2$ is a (2×2) matrix which defines the second order terms of the stable manifold approximation. Defining

$$O_2(R_u(u_1, u_2, 0)) = (u_1\ u_2)\,\mathbf{G}_2\begin{pmatrix}u_1\\u_2\end{pmatrix}, \quad (42)$$

then as shown by Venkatasubramanian and Ji [24], $\mathbf{H}_2$ may be determined from the equation:

$$\mathbf{H}_2(\lambda_u\mathbf{I} - 2\mathbf{A}_s) = -\mathbf{G}_2. \quad (43)$$

The matrix $(\lambda_u\mathbf{I} - 2\mathbf{A}_s)$ will always be invertible, and will be diagonal if all the eigenvalues of the Jacobian matrix $\mathbf{A}$ are real. The matrix $\mathbf{G}_2$ is in principle known since $R_u(u_1, u_2, 0)$ is a known function.

The third order terms in h are determined by solving equation (39). In order to do this, define:

$$h_3 = (u_1^2\ u_2^2)\,\mathbf{H}_3\begin{pmatrix}u_1\\u_2\end{pmatrix},\ O_3(R_u(u_1, u_2, h_2)) = (u_1^2\ u_2^2)\,\mathbf{G}_{3u}\begin{pmatrix}u_1\\u_2\end{pmatrix},$$

$$O_2(\mathbf{R}_s(u_1, u_2, 0)) = \begin{bmatrix}(u_1\ \ u_2)\,\mathbf{K}_1\begin{pmatrix}u_1\\u_2\end{pmatrix}\\ \\ (u_1\ \ u_2)\,\mathbf{K}_2\begin{pmatrix}u_1\\u_2\end{pmatrix}\end{bmatrix}. \quad (44)$$

The terms on the right-hand side of equation (39) may now be rewritten as follows:

$$\left(\frac{\partial h_3}{\partial u_1}\ \frac{\partial h_3}{\partial u_2}\right)\mathbf{A}_2\begin{pmatrix}u_1\\u_2\end{pmatrix}=(u_1^2\ u_2^2)\,\mathbf{H}_3^*\begin{pmatrix}u_1\\u_2\end{pmatrix},\ \left(\frac{\partial h_2}{\partial u_1}\ \frac{\partial h_2}{\partial u_2}\right)O_2(\mathbf{R}_s(u_1,u_2,0)=(u_1^2\ u_2^2)\,\bar{\mathbf{G}}_3\begin{pmatrix}u_1\\u_2\end{pmatrix},\quad(45)$$

where the (2×2) matrices $\mathbf{H}_3^*$ and $\bar{\mathbf{G}}_3$ are given by

$$\mathbf{H}_3^*=\begin{bmatrix}3h_{11}^{(3)}a_{11}+a_{21}h_{12}^{(3)} & (2a_{11}+a_{22})h_{12}^{(3)}+3a_{12}h_{11}^{(3)}+2a_{21}h_{21}^{(3)}\\ (a_{11}+2a_{22})h_{21}^{(3)}+2a_{12}h_{12}^{(3)}+3a_{21}h_{22}^{(3)} & 3h_{22}^{(3)}a_{22}+a_{12}h_{21}^{(3)}\end{bmatrix},\quad(46)$$

$$\bar{\mathbf{G}}_3=\begin{bmatrix}2h_{11}^{(2)}k_{11}^{(1)}+(h_{12}^{(2)}+h_{21}^{(2)})k_{11}^{(2)} & \{2h_{11}^{(2)}(k_{12}^{(1)}+k_{21}^{(1)})+2h_{22}^{(2)}k_{11}^{(2)}\\ & \quad+(h_{12}^{(2)}+h_{21}^{(2)})(k_{12}^{(2)}+k_{21}^{(2)}+k_{11}^{(1)})\}\\ \{2h_{22}^{(2)}(k_{12}^{(2)}+k_{21}^{(2)})+2h_{11}^{(2)}k_{22}^{(1)} & \\ \quad+(h_{12}^{(2)}+h_{21}^{(2)})(k_{12}^{(1)}+k_{21}^{(1)}+k_{22}^{(2)})\} & 2h_{22}^{(2)}k_{22}^{(2)}+(h_{12}^{(2)}+h_{21}^{(2)})k_{22}^{(1)}\end{bmatrix}\quad(47)$$

and a_{ij}, $h_{ij}^{(2)}$, $h_{ij}^{(3)}$, $k_{ij}^{(1)}$ and $k_{ij}^{(2)}$ denote the ijth elements of the matrices $\mathbf{A}$, $\mathbf{H}_2$, $\mathbf{H}_3$, $\mathbf{K}_1$ and $\mathbf{K}_2$ respectively. Equations (39) for the third order terms of h may then be written:

$$\lambda_u\mathbf{H}_3-\mathbf{H}_3^*=\bar{\mathbf{G}}_3-\mathbf{G}_{3u},\quad(48)$$

where $\bar{\mathbf{G}}_3$ is given by equation (47). $\mathbf{K}_1$, $\mathbf{K}_2$ and $\mathbf{G}_{3u}$ are in principle known since $\mathbf{R}_s(u_1,u_2,0)$ and $R_u(u_1,u_2,h_2)$ are known functions. $\mathbf{H}_3^*$, as may be seen from equation (46), is a function of the elements of $\mathbf{H}_3$. Substituting from equations (46) and (47) then results in four equations to determine the elements of $\mathbf{H}_3$. These may be written in the following form:

$$\begin{bmatrix}\lambda_u-3a_{11} & -a_{21} & 0 & 0\\ -3a_{12} & \lambda_u-2a_{11}-a_{22} & -2a_{21} & 0\\ 0 & -2a_{12} & \lambda_u-a_{11}-2a_{22} & -3a_{21}\\ 0 & 0 & -a_{12} & \lambda_u-3a_{22}\end{bmatrix}\begin{bmatrix}h_{11}^{(3)}\\h_{12}^{(3)}\\h_{21}^{(3)}\\h_{22}^{(3)}\end{bmatrix}=\begin{bmatrix}(\bar{\mathbf{G}}_3-\mathbf{G}_{3u})_{11}\\(\bar{\mathbf{G}}_3-\mathbf{G}_{3u})_{12}\\(\bar{\mathbf{G}}_3-\mathbf{G}_{3u})_{21}\\(\bar{\mathbf{G}}_3-\mathbf{G}_{3u})_{22}\end{bmatrix}.\quad(49)$$

The tri-diagonal matrix on the left-hand side of equation (49) will become diagonal if the matrix $\mathbf{A}_s$ is also diagonal.

The fourth order terms of h are determined by solving equations (40). To do this, write

$$h_4=(u_1^2\quad u_1u_2\quad u_2^2)\begin{pmatrix}h_{11}^{(4)} & 0 & 0\\ h_{21}^{(4)} & h_{22}^{(4)} & 0\\ 0 & h_{32}^{(4)} & h_{33}^{(4)}\end{pmatrix}\begin{pmatrix}u_1^2\\u_1u_2\\u_2^2\end{pmatrix}=(u_1^2\quad u_1u_2\quad u_2^2)\,\mathbf{H}_4\begin{pmatrix}u_1^2\\u_1u_2\\u_2^2\end{pmatrix}.\quad(50)$$

Furthermore, write

$$O_4(R_u(u_1,u_2,h_2+h_3))=(u_1^2\quad u_1u_2\quad u_2^2)\,\mathbf{G}_{4u}\begin{pmatrix}u_1^2\\u_1u_2\\u_2^2\end{pmatrix},$$

$$\left(\frac{\partial h_3}{\partial u_1}\ \frac{\partial h_3}{\partial u_2}\right)O_2(\mathbf{R}_s(u_1,u_2,0))=(u_1^2\ u_1u_2\ u_2^2)\,\mathbf{H}_4^{**}\begin{pmatrix}u_1^2\\u_1u_2\\u_2^2\end{pmatrix},$$

$$\left(\frac{\partial h_4}{\partial u_1}\ \frac{\partial h_4}{\partial u_2}\right)\mathbf{A}_s\begin{pmatrix}u_1\\u_2\end{pmatrix} = (u_1^2\ \ u_1u_2\ \ u_2^2)\,\mathbf{H}_4^*\begin{pmatrix}u_1^2\\u_1u_2\\u_2^2\end{pmatrix},$$

$$\left(\frac{\partial h_2}{\partial u_1}\ \frac{\partial h_2}{\partial u_2}\right)O_3(\mathbf{R}_s(u_1,u_2,h_2)) = (u_1^2\ \ u_1u_2\ \ u_2^2)\,\bar{\mathbf{H}}_4\begin{pmatrix}u_1^2\\u_1u_2\\u_2^2\end{pmatrix}, \tag{51}$$

where the matrices $\mathbf{G}_{4u}$, $\mathbf{H}_4^*$, $\mathbf{H}_4^{**}$ and $\bar{\mathbf{H}}_4$ are of the same form as $\mathbf{H}_4$, i.e., only the diagonal and sub-diagonal contain non-zero entries. $\mathbf{G}_{4u}$ is in principle known since $R_u(u_1, u_2, h_2 + h_3)$ is a known function. The non-zero elements of $\mathbf{H}_4^{**}$ may be determined by using equations (44) to give

$$\begin{aligned}
(\mathbf{H}_4^{**})_{11} &= 3h_{11}^{(3)}k_{11}^{(1)} + h_{12}^{(3)}k_{11}^{(2)},\\
(\mathbf{H}_4^{**})_{21} &= 3h_{11}^{(3)}(k_{12}^{(1)} + k_{21}^{(1)}) + h_{12}^{(3)}(k_{12}^{(2)} + k_{21}^{(2)}) + 2h_{12}^{(3)}k_{11}^{(1)} + 2h_{21}^{(3)}k_{11}^{(2)},\\
(\mathbf{H}_4^{**})_{22} &= h_{21}^{(3)}k_{11}^{(1)} + 3h_{12}^{(3)}k_{11}^{(2)} + 3h_{11}^{(3)}k_{22}^{(1)} + h_{12}^{(3)}k_{22}^{(2)} + 2h_{12}^{(3)}(k_{12}^{(1)} + k_{21}^{(1)}) + 2h_{21}^{(3)}(k_{12}^{(2)} + k_{21}^{(2)}),\\
(\mathbf{H}_4^{**})_{32} &= h_{21}^{(3)}(k_{12}^{(1)} + k_{21}^{(1)}) + 3h_{22}^{(3)}(k_{12}^{(2)} + k_{21}^{(2)}) + 2h_{12}^{(3)}k_{22}^{(1)} + 2h_{21}^{(3)}k_{22}^{(2)},\\
(\mathbf{H}_4^{**})_{33} &= h_{21}^{(3)}k_{22}^{(1)} + 3h_{22}^{(3)}k_{22}^{(2)}.
\end{aligned} \tag{52}$$

The non-zero elements of $\mathbf{H}_4^*$ are given by

$$\begin{aligned}
(\mathbf{H}_4^{*})_{11} &= 4a_{11}h_{11}^{(4)} + a_{21}h_{12}^{(4)},\\
(\mathbf{H}_4^{*})_{21} &= 3a_{11}h_{21}^{(4)} + 4a_{12}h_{11}^{(4)} + 2a_{21}h_{22}^{(4)} + h_{21}^{(4)}a_{22},\\
(\mathbf{H}_4^{*})_{22} &= 2a_{11}h_{22}^{(4)} + 3a_{12}h_{21}^{(4)} + 3a_{21}h_{32}^{(4)} + 2a_{22}h_{22}^{(4)},\\
(\mathbf{H}_4^{*})_{32} &= a_{11}h_{32}^{(4)} + 2a_{12}h_{22}^{(4)} + 4a_{21}h_{33}^{(4)} + 3a_{22}h_{32}^{(4)},\\
(\mathbf{H}_4^{*})_{33} &= a_{12}h_{32}^{(4)} + 4a_{22}h_{33}^{(4)}.
\end{aligned} \tag{53}$$

The matrix $\bar{\mathbf{H}}_4$ may be determined by first writing

$$O_3(\mathbf{R}_s(u_1,u_2,h_2)) = \begin{bmatrix}(u_1^2\ \ u_2^2)\,\mathbf{L}_1\begin{pmatrix}u_1\\u_2\end{pmatrix}\\[2ex](u_1^2\ \ u_2^2)\,\mathbf{L}_2\begin{pmatrix}u_1\\u_2\end{pmatrix}\end{bmatrix} = \begin{bmatrix}l_{11}^{(1)}u_1^3 + l_{12}^{(1)}u_1^2u_2 + l_{21}^{(1)}u_1u_2^2 + l_{22}^{(1)}u_2^3\\ l_{11}^{(2)}u_1^3 + l_{12}^{(2)}u_1^2u_2 + l_{21}^{(2)}u_1u_2^2 + l_{22}^{(2)}u_2^3\end{bmatrix} \tag{54}$$

where the coefficients $l_{11}^{(1)}, l_{12}^{(1)}, \ldots$ and $l_{11}^{(2)}, l_{12}^{(2)}, \ldots$ are the elements of $\mathbf{L_1}$ and $\mathbf{L_2}$ respectively. $\mathbf{L_1}$ and $\mathbf{L_2}$ are in principle known as $\mathbf{R}_s(u_1, u_2, h_2)$ is known. Then the non-zero elements of $\bar{\mathbf{H}}_4$ are given by

$$\begin{aligned}
(\bar{\mathbf{H}}_4)_{11} &= 2h_{11}^{(2)}l_{11}^{(1)} + (h_{12}^{(2)} + h_{21}^{(2)})\ l_{11}^{(2)},\\
(\bar{\mathbf{H}}_4)_{21} &= 2h_{11}^{(2)}l_{12}^{(1)} + (h_{12}^{(2)} + h_{21}^{(2)})\ l_{11}^{(1)} + 2h_{22}^{(2)}l_{11}^{(2)} + (h_{12}^{(2)} + h_{21}^{(2)})\ l_{12}^{(2)},\\
(\bar{\mathbf{H}}_4)_{22} &= 2h_{11}^{(2)}l_{21}^{(1)} + (h_{12}^{(2)} + h_{21}^{(2)})\ l_{12}^{(1)} + 2h_{22}^{(2)}l_{12}^{(2)} + (h_{12}^{(2)} + h_{21}^{(2)})\ l_{21}^{(2)},\\
(\bar{\mathbf{H}}_4)_{32} &= 2h_{11}^{(2)}l_{22}^{(1)} + (h_{12}^{(2)} + h_{21}^{(2)})\ l_{21}^{(1)} + 2h_{22}^{(2)}l_{21}^{(2)} + (h_{12}^{(2)} + h_{21}^{(2)})\ l_{22}^{(2)},\\
(\bar{\mathbf{H}}_4)_{33} &= (h_{12}^{(2)} + h_{21}^{(2)})\ l_{22}^{(1)} + 2h_{22}^{(2)}l_{22}^{(2)}.
\end{aligned} \tag{55}$$

Equation (40) for the fourth order terms of h may then be written:

$$\lambda_u\mathbf{H}_4 - \mathbf{H}_4^* = \bar{\mathbf{H}}_4 - \mathbf{G}_{4u} + \mathbf{H}_4^{**}, \tag{56}$$

where $\mathbf{G}_{4u}$, $\mathbf{H}_4^{**}$ and $\bar{\mathbf{H}}_4$ are known but $\mathbf{H}_4^{*}$ is a function of the elements of $\mathbf{H}_4$. Substituting from equations (52), (53) and (55) in equations (56) then results in five equations to determine the non-zero elements of $\mathbf{H}_4$. These may be written in the following form:

$$\begin{bmatrix} \lambda_u - 4a_{11} & -a_{21} & 0 & 0 & 0 \\ -4a_{12} & \lambda_u - 3a_{11} - a_{22} & -2a_{21} & 0 & 0 \\ 0 & -3a_{12} & \lambda_u - 2a_{11} - 2a_{22} & -3a_{21} & 0 \\ 0 & 0 & -2a_{12} & \lambda_u - a_{11} - 3a_{12} & -4a_{21} \\ 0 & 0 & 0 & -a_{12} & \lambda_u - 4a_{22} \end{bmatrix} \begin{Bmatrix} h_{11}^{(4)} \\ h_{21}^{(4)} \\ h_{22}^{(4)} \\ h_{32}^{(4)} \\ h_{33}^{(4)} \end{Bmatrix}$$

$$= \begin{Bmatrix} (\bar{\mathbf{H}}_4 - \mathbf{G}_{4u} + \mathbf{H}_4^{**})_{11} \\ (\bar{\mathbf{H}}_4 - \mathbf{G}_{4u} + \mathbf{H}_4^{**})_{21} \\ (\bar{\mathbf{H}}_4 - \mathbf{G}_{4u} + \mathbf{H}_4^{**})_{22} \\ (\bar{\mathbf{H}}_4 - \mathbf{G}_{4u} + \mathbf{H}_4^{**})_{32} \\ (\bar{\mathbf{H}}_4 - \mathbf{G}_{4u} + \mathbf{H}_4^{**})_{33} \end{Bmatrix}. \tag{57}$$

Equations (43), (49) and (57) determine the matrices $\mathbf{H}_2$, $\mathbf{H}_3$ and $\mathbf{H}_4$ that define the stable manifold up to fourth order. However, evaluation of the matrices $\mathbf{G}_2$, $\mathbf{G}_{3u}$, $\mathbf{G}_{4u}$, $\mathbf{K}_1$, $\mathbf{K}_2$, $\mathbf{L}_1$, $\mathbf{L}_2$ has not been discussed although it has been noted that they can in principle be determined. All of these matrices may be determined by Taylor series expansions in u_1 and u_2 of $R_u(u_1, u_2, 0)$, $R_u(u_1, u_2, h_2)$, $R_u(u_1, u_2, h_2 + h_3)$, $\mathbf{R}_s(u_1, u_2, 0)$ and $\mathbf{R}_s(u_1, u_2, h_2)$, which will require calculating partial derivatives of these functions up to fourth order. One approach to this might be through the use of a computer algebra package to evaluate the derivatives analytically. Alternatively, they can be evaluated numerically by finite differences; however, this approach can encounter difficulties for higher derivatives. The approach adopted here was to evaluate first derivatives analytically, which was necessary to obtain the Jacobian matrix $\mathbf{A}$, and then to determine higher derivatives by second order finite differences based on the first derivatives. Thus, only third derivatives at most were calculated numerically, and this procedure proved stable and simple to implement. However, if further terms of the stable manifold expansion are desired, computer algebra, or alternatively the use of automatic differentiation to determine the required derivatives, would offer the only viable means.

5. RESULTS

In this section, two examples of the use of the analysis of sections 3 and 4 in predictions of the domain of attraction of the stable equilibrium point O for an all-moving control surface in supersonic flow, whose aeroelastic behaviour is governed by equations (15), are given. Both cases consider a control surface for which full details are given in Appendix A. Given there are the geometric characteristics together with the natural modes and associated generalized masses and stiffnesses in the case when the root attachment torsional stiffness is zero. This modal data was derived from a finite element model of the lifting surface. For the determination of the aerodynamic loadings on the control surface, thickness effects were neglected. Flight is assumed to take place under sea level international standard atmosphere conditions.

The first example considers a case where the control surface possesses a cubic hardening non-linearity in the root torsional degree of freedom. Thus, the moment M_y in equation (2)

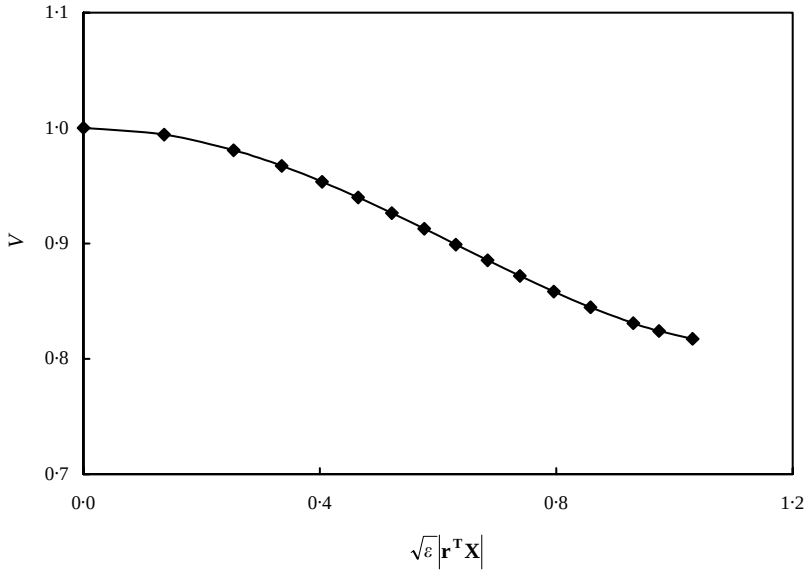

Figure 4. Variation of limit cycle amplitude with non-dimensionalized speed V for System I.

may be written:

$$M_y = -Kr^{\mathrm{T}}X - \varepsilon K(r^{\mathrm{T}}X)^3, \tag{58}$$

where K is the linear torsional spring constant. In formulating the aeroelastic equations, the linear terms arising from equation (58) were incorporated into the matrix **H**. Thus, the function f could be written:

$$f(\mathbf{r}^{\mathrm{T}}\mathbf{X}) = K(\mathbf{r}^{\mathrm{T}}\mathbf{X})^3. \tag{59}$$

In this example K was taken as 75·9 N m/rad. The flutter speed of the linear system ($\varepsilon = 0$) was first determined and speed was then non-dimensionalized with respect to this. Additionally, a non-dimensional time $t' = \tilde{\omega}t$ was defined so that the flutter frequency of the linear system would be O(1). To achieve this the value of $\tilde{\omega}$ was taken as 1800 rad/s. The matrices **G**, **H** and vectors **r**, **s** that define the aeroelastic equations for the control surface could then be evaluated, using the data of Appendix A, to be

$$\begin{aligned}
\mathbf{G} &= \begin{bmatrix} 1{\cdot}84329 \times 10^{-2} & 2{\cdot}48859 \times 10^{-3} \\ 3{\cdot}98055 \times 10^{-4} & 1.81111 \times 10^{-2} \end{bmatrix}, \\
\mathbf{H} &= \begin{bmatrix} 0{\cdot}16727V + 0{\cdot}42110 & 0{\cdot}16820V + 0{\cdot}49896 \\ -0{\cdot}24317V + 7{\cdot}98092 \times 10^{-2} & 1{\cdot}31621 - 0{\cdot}25748V \end{bmatrix}, \\
\mathbf{r} &= \begin{bmatrix} 1{\cdot}0 \\ 1{\cdot}18488 \end{bmatrix}, \quad \mathbf{s} = \begin{bmatrix} 0{\cdot}421104 \\ 7{\cdot}98092 \times 10^{-2} \end{bmatrix},
\end{aligned} \tag{60}$$

where V is the non-dimensional speed defined as explained previously such that $V = 1{\cdot}0$ is the flutter speed for the linear system. The matrix **G** gives the aerodynamic damping terms and is independent of speed. This arises because control surface thickness effects have been neglected in the aerodynamics. Thus, the integrals I_{1s}, I_{2s}, I_{3s}, I_{4s} and I_{5s} are zero so that the coefficients I_{ij} in equation (14) may be readily shown to be independent of speed. The system defined by equations (60) will be referred to as System I.

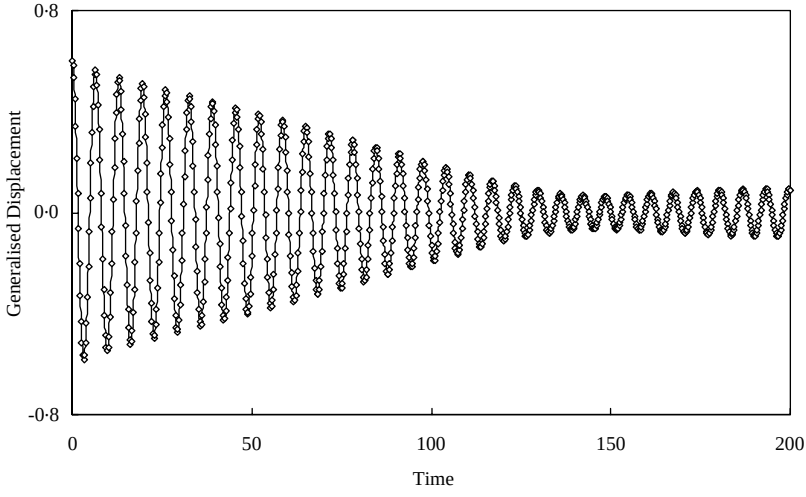

Figure 5. Predictions of response in X_1 for System I, $\varepsilon = 0{\cdot}025$, $V = 0{\cdot}99431$, initial conditions: $X_1^{(0)} = 0{\cdot}6$, $X_2^{(0)} = 0{\cdot}3$, $\dot{X}_1^{(0)} = 0{\cdot}0$, $\dot{X}_2^{(0)} = 0{\cdot}0$; ——, aeroelastic equation (15); $\diamond$, averaged equations (31).

TABLE 1

Values of λ_1, λ_2, ω_1, and ω_2 for the averaged form of equations for System I

V	λ_1	λ_2	ω_1	ω_2	$\omega_1 - \omega_2$
0·99431	− 0·0106531	− 0·0076189	0·937020	0·979064	− 0·042044
0·95345	− 0·0095943	− 0·0086777	0·892889	1·021280	− 0·128391
0·88535	− 0·0093851	− 0·0088869	0·853998	1·056940	− 0·202942

Prior to any domain of stability investigations, a study was carried out to investigate the non-linear aeroelastic behaviour of the system for $\varepsilon > 0$ in terms of the existence of possible limit cycles and their stability. The limit cyces were determined by the harmonic balance method. Figure 4 shows the variation of limit cycle amplitude with flight speed plotted in terms of $\sqrt{\varepsilon}|\mathbf{r}^{\mathrm{T}}\mathbf{X}|$ against V. These results were checked using numerical integration in the time domain, and for small values of $\sqrt{\varepsilon}|\mathbf{r}^{\mathrm{T}}\mathbf{X}|$ using the averaging method. This also confirmed that the limit cycles were unstable. Thus, $V = 1{\cdot}0$ is the speed at which sub-critical Hopf bifurcation occurs for the non-linear system, with O being stable for $V < 1{\cdot}0$.

For the initial study with System I, $\varepsilon = 0{\cdot}025$ and $V = 0{\cdot}99431$; thus the non-linearity is weak and the air-flow speed is very close to the linear flutter speed. The choice of value for ε then implied that $\mathbf{r}^{\mathrm{T}}\mathbf{X}$ should be regarded as being proportional to, rather than equal to, the root torsion angle θ_y. As a check on the accuracy of the averaging procedure, comparisons were made between aeroelastic response predictions from equation (15) and the averaged equations (31) with the integrals evaluated using f as given in equation (59) above. Comparisons for initial conditions $\mathbf{X} = (0{\cdot}6, 0{\cdot}3)^{\mathrm{T}}$, $\dot{\mathbf{X}} = \mathbf{0}$ are shown in Figure 5 for non-dimensionalized time $0 < t' < 200$. Agreement may be seen to be good. Values of λ_1, λ_2,

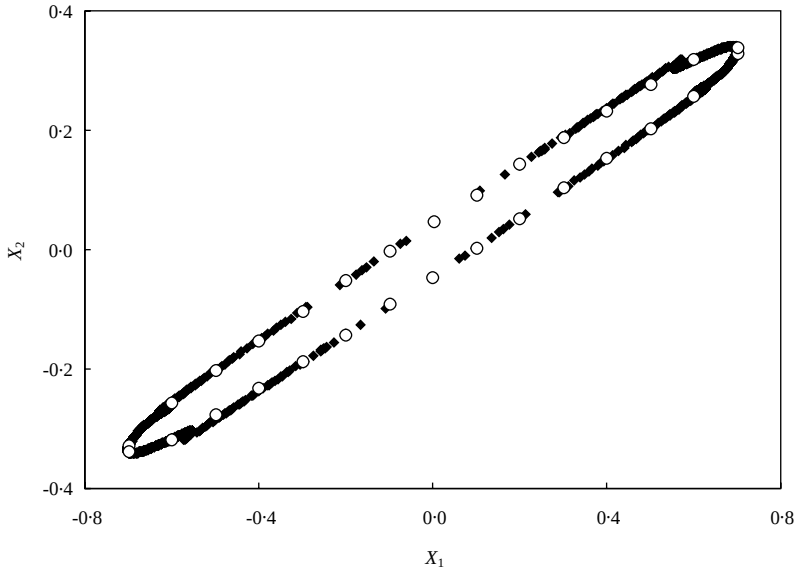

Figure 6. Domain of attraction for System I, $\varepsilon = 0{\cdot}025$, $V = 0{\cdot}99431$, initial conditions: $\dot{X}_1^{(0)} = 0{\cdot}0$, $\dot{X}_2^{(0)} = 0{\cdot}0$; ○, time domain prediction; ◆, stable manifold analysis.

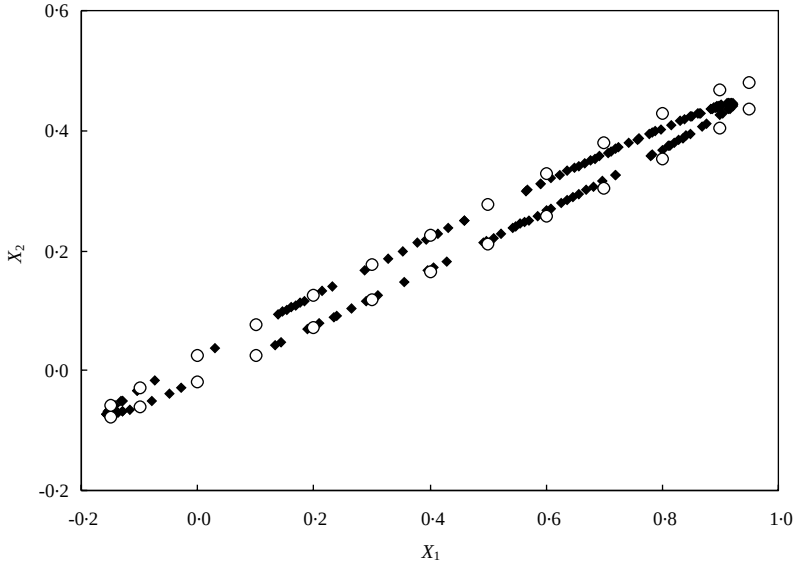

Figure 7. Domain of attraction for System I, $\varepsilon = 0{\cdot}025$, $V = 0{\cdot}99431$, initial conditions: $\dot{X}_1^{(0)} = 0{\cdot}08$, $\dot{X}_2^{(0)} = 0{\cdot}0$; ○, time domain prediction; ◆, stable manifold analysis.

ω_1 and ω_2 in the averaged equations (31) are shown in Table 1, from which it may be seen that λ_1, λ_2 and $\omega_1 - \omega_2$ are small, as required.

The domain of attraction of O was then investigated. First, the fixed point of the averaged equations (31) corresponding to the unstable limit cycle had to be determined. This was done numerically by first locating the limit cycle from equation (15) by using the method of harmonic balance. The result was then translated into the averaged variables A_1, A_2, θ and

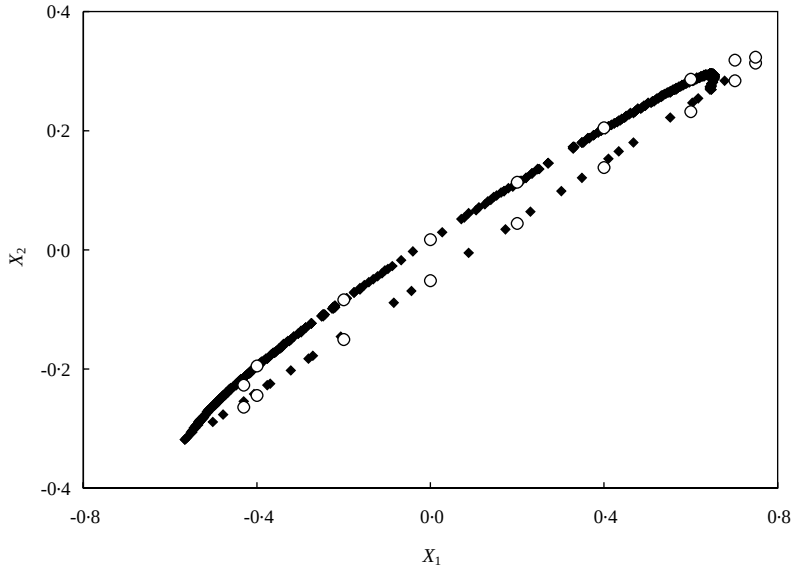

Figure 8. Domain of attraction for System I, $\varepsilon = 0{\cdot}025$, $V = 0{\cdot}99431$, initial conditions: $\dot{X}_1^{(0)} = -0{\cdot}5$, $\dot{X}_2^{(0)} = -0{\cdot}25$; ○, time domain prediction; ◆, stable manifold analysis.

this was used as an initial estimate of the required fixed point of equations (31). This estimate was then refined to give (A_1^0, A_2^0, θ^0). The Jacobian matrix **A** was then determined and the eigenvalues calculated to confirm that (A_1^0, A_2^0, θ^0) was an unstable point with a two-dimensional stable manifold. The matrices $\mathbf{H}_2$, $\mathbf{H}_3$ and $\mathbf{H}_4$ defining the stable manifold up to fourth order were then determined. Comparisons were made with predictions obtained by numerically integrating equation (15) for given initial values $X_1 = X_1^{(0)}$, $X_2 = X_2^{(0)}$, $\dot{X}_1 = \dot{X}_1^{(0)}$, $\dot{X}_2 = \dot{X}_2^{(0)}$. To obtain corresponding predictions from the stable manifold analysis, it should first be noted that by making use of equations (22), (24) and (26), $\dot{X}_1$ and $\dot{X}_2$ may be related to A_1, A_2 and θ by

$$\frac{\dot{\mathbf{X}}}{\sqrt{2}} = \mathrm{Re}(\mathbf{M}\boldsymbol{\mu})\begin{pmatrix} A_1 \sin\psi_1 \\ A_2 \sin(\psi_1 + \theta) \end{pmatrix} + \mathrm{Im}(\mathbf{M}\boldsymbol{\mu})\begin{pmatrix} A_1 \cos\psi_1 \\ A_2 \cos(\psi_1 + \theta) \end{pmatrix}. \tag{61}$$

The stable manifold can be determined in the neighbourhood of (A_1^0, A_2^0, θ^0) as u_1, u_2 are varied and the corresponding values of A_1, A_2 and θ evaluated. Then for the given value $\dot{X}_1^{(0)}$ of $\dot{X}_1$, the first of equations (61) may be solved for ψ_1. If a solution is found, the second equation may be checked to see how near the resulting value of $\dot{X}_2$ is to a given value $\dot{X}_2^{(0)}$. If $|\dot{X}_2^{(0)} - \dot{X}_2|$ is within some specified small tolerance, the initial values $X_1^{(0)}$, $X_2^{(0)}$ of X_1, X_2 lying on the boundary of the stability domain may be determined from

$$\mathbf{X} = \sqrt{2}\ \mathrm{Re}(\mathbf{M})\begin{pmatrix} A_1 \sin\psi_1 \\ A_2 \sin(\psi_1 + \theta) \end{pmatrix} + \sqrt{2}\ \mathrm{Im}(\mathbf{M})\begin{pmatrix} A_1 \cos\psi_1 \\ A_2 \cos(\psi_1 + \theta) \end{pmatrix}, \tag{62}$$

this relation again being obtained from equations (22), (24) and (26).

Comparisons of the domain of attraction of O are shown in Figure 6 for $\dot{X}_1^{(0)} = 0$ and $\dot{X}_2^{(0)} = 0$. In the legend, "Time Domain Prediction" refers to numerical integration of equation (15). Agreement may be seen to be very good. Figures 7 and 8 show similar comparisons for initial conditions $\dot{X}_1^{(0)} = 0{\cdot}08$ and $\dot{X}_2^{(0)} = 0{\cdot}0$, and $\dot{X}_1^{(0)} = -0{\cdot}5$ and $\dot{X}_2^{(0)} = -0{\cdot}25$ respectively. Again, a good level of agreement is evident. Comparisons of

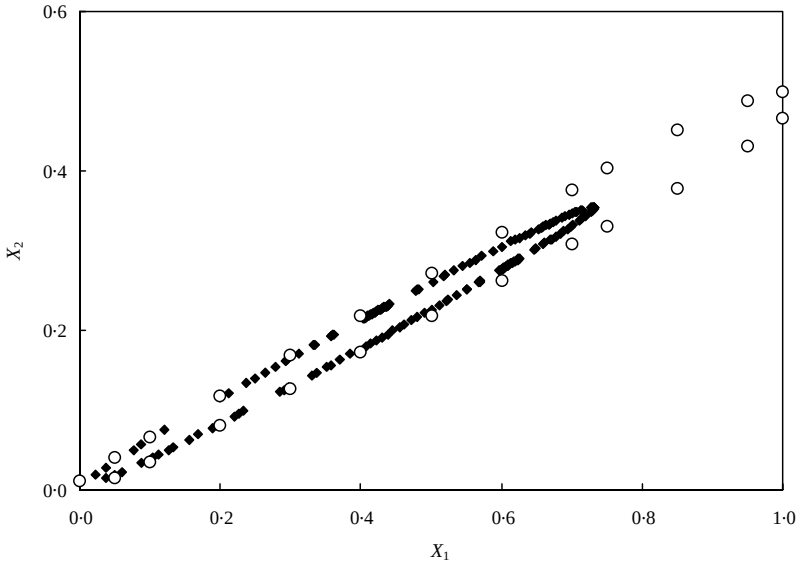

Figure 9. Domain of attraction for System I, $\varepsilon = 0{\cdot}025$, $V = 0{\cdot}99431$, initial conditions: $\dot{X}_1^{(0)} = 0{\cdot}09$, $\dot{X}_2^{(0)} = 0{\cdot}0$; ○, time domain prediction; ◆, stable manifold analysis.

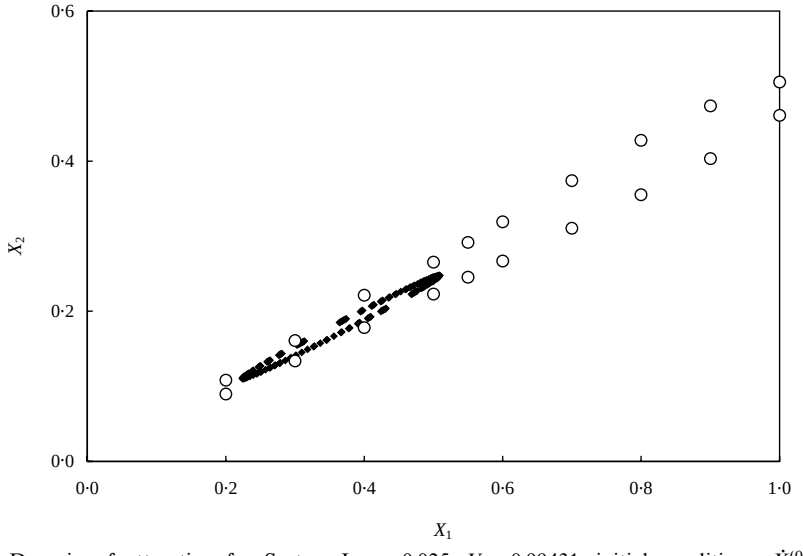

Figure 10. Domain of attraction for System I, $\varepsilon = 0{\cdot}025$, $V = 0{\cdot}99431$, initial conditions: $\dot{X}_1^{(0)} = 0{\cdot}09625$ $\dot{X}_2^{(0)} = 0{\cdot}0$; ○, time domain prediction; ◆, stable manifold analysis.

Figures 6 and 7 indicate how the domain of attraction can be very sensitive to small variations in $\dot{X}_1^{(0)}$ and $\dot{X}_2^{(0)}$. The fact that the stable manifold analysis is only locally valid is illustrated by Figures 7, 9 and 10. Figure 7, as already mentioned, shows good agreement between domain of attraction predictions for $\dot{X}_1^{(0)} = 0{\cdot}08$ and $\dot{X}_2^{(0)} = 0{\cdot}0$, but as $\dot{X}_1^{(0)}$ increases first to 0.09 and then to 0·09625, agreement rapidly deteriorates with the predictions based on the stable manifold analysis of the averaged equations being

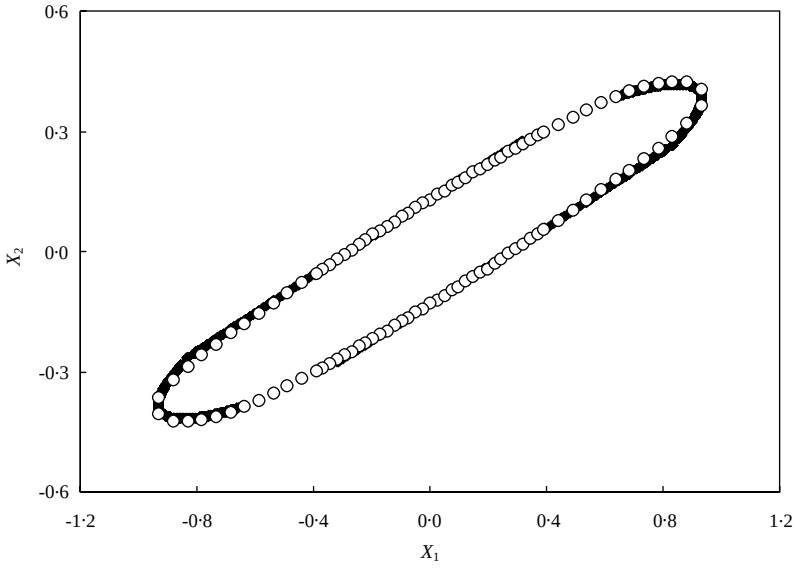

Figure 11. Domain of attraction for System I, $\varepsilon = 0{\cdot}10$, $V = 0{\cdot}95345$, initial conditions: $\dot{X}_1^{(0)} = 0{\cdot}0$, $\dot{X}_2^{(0)} = 0{\cdot}0$; ○, time domain prediction; ◆, stable manifold analysis.

conservative. For a further increase in $\dot{X}_1^{(0)}$ to 0·0975, the latter method predicts that the domain of attraction disappears altogether in contrast with time domain analysis.

The effect of reducing flow speed V was next considered for System I. The consequence of doing this will be to increase the amplitude of motion of the unstable limit cycle of the system, as shown in Figure 4, so that the domain of attraction of O will be larger. Thus, the non-linear effect will be more significant. In the following study, ε was set equal to 0·1; the effect of doing this being to rescale the domain of attraction of O. Figures 11 and 12 show the effect of reducing V for initial conditions $\dot{X}_1^{(0)} = 0$ and $\dot{X}_2^{(0)} = 0$. Table 1 shows values of λ_1, λ_2, ω_1 and ω_2 in the averaged equations for the values of V considered and again, λ_1, λ_2 and $\omega_1 - \omega_2$ are small, as required. Good agreement is obtained in Figure 11 for $V = 0{\cdot}95345$; and in Figure 12 for $V = 0{\cdot}88535$ although the stable manifold analysis of the averaged equations has produced some extra points as shown. These results indicate that the averaged form of the equations remain a good approximation to the original system (15) but suggest that further terms in the stable manifold expansion may be desirable.

The second example considers the case where the control surface possesses a freeplay non-linearity in the root torsional degree of freedom. Whereas System I was perhaps a somewhat theoretical example, the freeplay non-linearity is commonly encountered in practice and a number of previous investigations of non-linear aeroelastic systems have involved structures with freeplay non-linearities [1–9, 14, 16]. Furthermore, this non-linearity comes under the area of piecewise linear systems, which have themselves been a subject of considerable research [26–32]. One way of defining the freeplay non-linearity is by writing

$$\varepsilon f(\mathbf{r}^{\mathrm{T}}\mathbf{X}) = \begin{cases} K(\mathbf{r}^{\mathrm{T}}\mathbf{X} + \delta), & \mathbf{r}^{\mathrm{T}}\mathbf{X} < -\delta, \\ 0, & -\delta < \mathbf{r}^{\mathrm{T}}\mathbf{X} < \delta, \\ \mathrm{K}(\mathbf{r}^{\mathrm{T}}\mathbf{X} - \delta), & \mathbf{r}^{\mathrm{T}}\mathbf{X} > \delta, \end{cases} \tag{63}$$

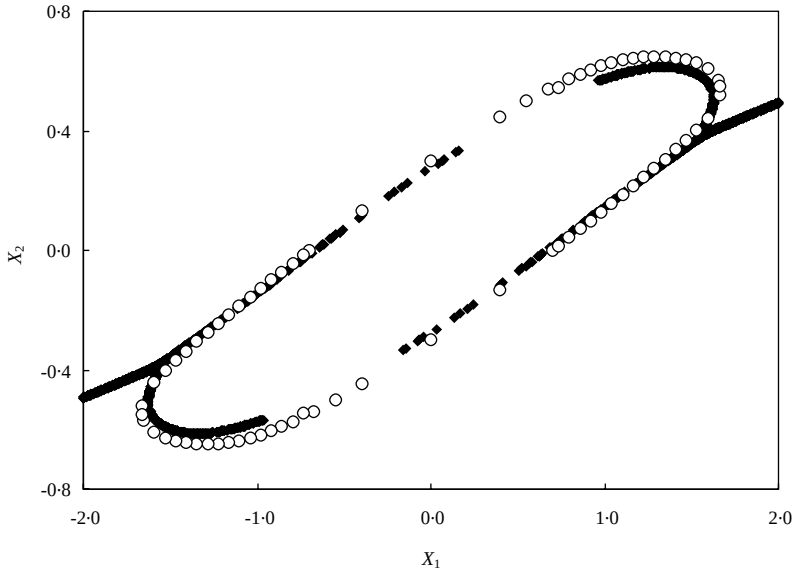

Figure 12. Domain of attraction for System I, $\varepsilon = 0{\cdot}10$, $V = 0{\cdot}88535$, initial conditions: $\dot{X}_1^{(0)} = 0{\cdot}0$, $\dot{X}_2^{(0)} = 0{\cdot}0$; ○, time domain prediction; ◆, stable manifold analysis.

where δ denotes the degree of freeplay and K is the linear stiffness. However, for this study, it is more appropriate to include the linear root torsional stiffness terms with the matrix **H**, rather as was done for System I, and to define the freeplay non-linearity by

$$\varepsilon f(\mathbf{r}^{\mathrm{T}}\mathbf{X}) = \begin{cases} K\delta, & \mathbf{r}^{\mathrm{T}}\mathbf{X} < -\delta, \\ -K\mathbf{r}^{\mathrm{T}}\mathbf{X}, & -\delta < \mathbf{r}^{\mathrm{T}}\mathbf{X} < \delta, \\ -K\delta, & \mathbf{r}^{\mathrm{T}}\mathbf{X} > \delta. \end{cases} \tag{64}$$

The lifting surface geometric, inertial and structural characteristics are again as given in Appendix A. However, in this example K was now taken as 151·8 N m/rad. The flutter speed of the linear system ($\delta = 0$) was first determined and speed was then non-dimensionalized with respect to this. In a manner similar to the cubic non-linearity, a non-dimensional time $t' = \tilde{\omega}$t was defined so that the flutter frequency of the linear system would be of O(1). To achieve this the value of $\tilde{\omega}$ was taken as 1940 rad/s. The matrices **G**, **H** and vectors **r**, **s** that define the aeroelastic equations for the control surface could then be evaluated, and in terms of non-dimensional speed V, are as follows:

$$\mathbf{G} = \begin{bmatrix} 1{\cdot}71027 \times 10^{-2} & 2{\cdot}30900 \times 10^{-3} \\ 3{\cdot}69330 \times 10^{-4} & 1{\cdot}68041 \times 10^{-2} \end{bmatrix},$$

$$\mathbf{H} = \begin{bmatrix} 0{\cdot}11701V + 0{\cdot}72504 & 0{\cdot}11757V + 0{\cdot}85909 \\ -0{\cdot}16998V + 0{\cdot}13741 & 1{\cdot}37732 - 0{\cdot}17999V \end{bmatrix},$$

$$\mathbf{r} = \begin{bmatrix} 1{\cdot}0 \\ 1{\cdot}18488 \end{bmatrix}, \qquad \mathbf{s} = \begin{bmatrix} 0{\cdot}72504 \\ 0{\cdot}13741 \end{bmatrix}. \tag{65}$$

This set of equations will be defined as System II. As in System I, the matrix **G** is independent of speed.

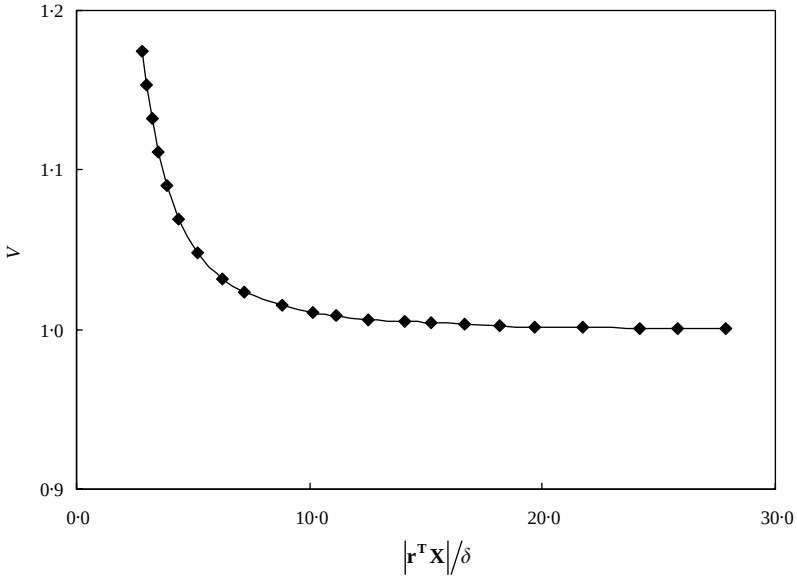

Figure 13. Limit cycle amplitude versus non-dimensionalized speed for System II.

As for System I, prior to any domain of stability investigations, a study was carried out to investigate the non-linear aeroelastic behaviour of System II in terms of the existence of possible limit cycles and their stability. The limit cycles again were determined by the harmonic balance method. Figure 13 shows the variation of limit cycle amplitude with flight speed expressed in terms of $|\mathbf{r}^T\mathbf{X}|/\delta$ against V. These results were also checked using numerical integration in the time domain, and for large values of $|\mathbf{r}^T\mathbf{X}|/\delta$ using the averaging method. This also confirmed that the limit cycles were unstable. Thus $V = 1{\cdot}0$ is the speed beyond which unstable limit cycles first occur, and as V increases, their amplitudes decrease, while O is stable for all V. As is clear from Figure 13, just above the linear flutter speed, the limit cycle is of large amplitude relative to δ; the domain of attraction of O might be expected to be large relative to δ, and thus in the analysis to determine the domain of attraction, the system can be regarded as weakly non-linear. Furthermore, the limit cycle amplitude will decrease rapidly for small increments in V immediately beyond $V = 1{\cdot}0$. As speed increases, the system may be thought of as being more strongly non-linear. It should be noted that the non-linearity is defined by a function that has discontinuous derivatives. Nevertheless, the averaged system will be continuous and many-times differentiable in the neighbourhood of the unstable equilibrium point corresponding to the unstable limit cycle of the original system (15). Thus, the stable manifold may be obtained by power series expansion as before.

For the first case considered, $V = 1{\cdot}000167$. Comparisons of the domain of attraction as predicted by numerical integration of equation (15) and stable manifold analysis of the averaged equations (31) are shown in Figure 14 for initial conditions $\dot{X}_1^{(0)} = 0$ and $\dot{X}_2^{(0)} = 0$. In Figure 14, displacements are again expressed as a factor of δ. It may be seen that there is a fair degree of agreement although the results from the stable manifold analysis overestimate the size of the domain of attraction. Figure 15 shows results for $V = 1{\cdot}00646$. In this case, agreement between the two methods is very good. Although the increase in V from Figure 14 is very small, the reduction in size of the domain of attraction of O is very significant. This is consistent with the behaviour of the limit cycle amplitude of the system as

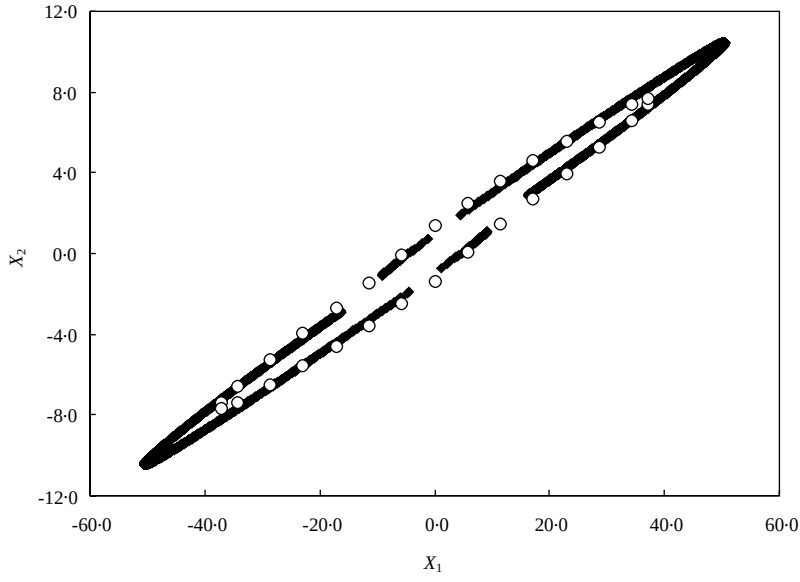

Figure 14. Domain of attraction for System II, $V = 1{\cdot}0001668$, initial conditions: $\dot{X}_1^{(0)} = 0{\cdot}0$, $\dot{X}_2^{(0)} = 0{\cdot}0$; ○, time domain prediction; ◆, stable manifold analysis.

shown in Figure 13, and this sensitivity is the most likely explanation for the discrepancies in Figure 14. Figure 16 shows the domain of attraction of O as speed V is further increased up to 1·0903. A good level of agreement between time domain and stable manifold analysis of the averaged equations is again obtained. As speed increases, the non-linearity may in effect be regarded as becoming stronger. The results indicate both that the accuracy of the averaging method and the degree of approximation of the stable manifold adopted are sufficient to enable significant information about the domain of attraction of the equilibrium point to be obtained for System II.

Table 2 shows values of λ_1, λ_2, ω_1 and ω_2 in the averaged equations for the values of V considered in this study of System II, and as is shown, λ_1, λ_2 and $\omega_1 - \omega_2$ are small as required.

6. CONCLUDING REMARKS

In this paper, the aeroelastic behaviour at high Mach numbers of an all-moving control surface with a non-linearity in the root support has been investigated. The particular situation investigated is that where a stable equilibrium point, corresponding to zero displacement of the structure, together with an unstable limit cycle typically arising from a sub-critical Hopf bifurcation results from the presence of the non-linearity so that the stable equilibrium point will then possess a domain of attraction. The approach adopted has been to first apply the averaging method to obtain a new set of aeroelastic equations in which the limit cycle is replaced by an unstable equilibrium point. A fourth order expansion of the stable manifold for this equilibrium point was carried out from which predictions of the domain of attraction of the stable equilibrium point were then obtained. The method was applied to two examples in which the non-linearity was due to either a cubic hardening restoring moment or the presence of freeplay in the root support. Agreement was shown to

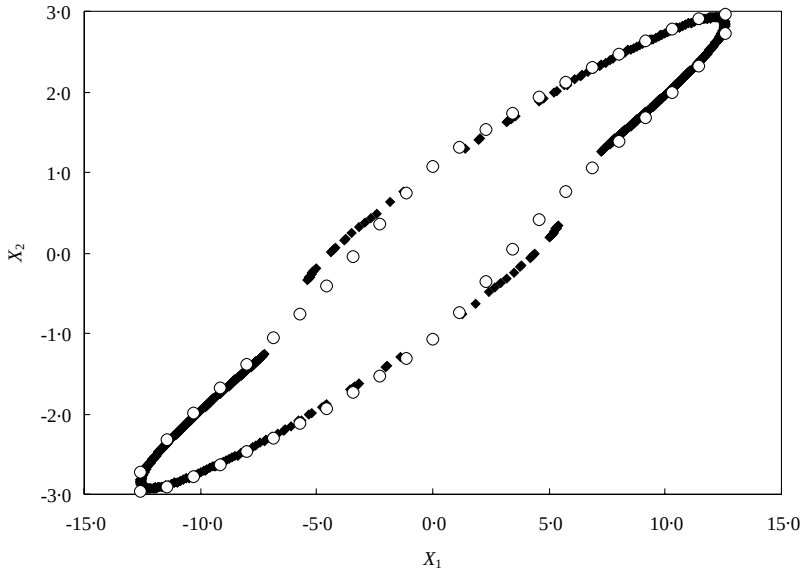

Figure 15. Domain of attraction for System II, $V = 1{\cdot}0064572$, initial conditions: $\dot{X}_1^{(0)} = 0{\cdot}0$, $\dot{X}_2^{(0)} = 0{\cdot}0$; ○, time domain prediction; ◆, stable manifold analysis.

be generally good in the cases considered. The averaging method adopted was shown to be sufficiently accurate for this analysis even when the non-linear effect could be regarded as strong.

The method of analysis used here has been shown to be effective in enabling a good indication of the extent of the stability domain to be obtained rapidly. The results have demonstrated the validity of the stable manifold analysis by comparisons with time domain numerical integration of the original system of equations. As the stable manifold expansions are only locally valid, it is important to have confidence that the domain of attraction has been determined from within the region of validity. One way to confirm, for example, that an nth order expansion is valid would be to compare the results with those from an $(n + 1)$th order expansion and to look for where the two expansions show agreement. In determining higher order terms, one difficulty that will be encountered is in obtaining Taylor series expansions of the terms $\mathbf{R}_s$ and R_u. Up to fourth order, it was found that calculating first derivatives analytically, which was necessary in order to obtain the Jacobian matrix $\mathbf{A}$, and then determining higher derivatives using second order finite differences based on the first derivatives was effective. It avoided cumbersome algebra and was numerically stable. Going to higher order would require more analytically determined derivatives, and this would best be carried out either using computer algebra or possibly through automatic differentiation. Although this study considered only one non-linearity; the approach used here could equally be used for aeroelastic systems with multiple structural non-linearities. The non-linearities considered here have been symmetric; again the approach could also be applied to non-symmetric non-linearities that typically arise when there is a pre-load present, for example, when the control surface is at an incidence to the flow in the steady state. Although the aeroelastic problem considered here is a practical one, the use of piston theory aerodynamics makes possible significant simplifications to the equations of motion. For flight regimes other than the high supersonic, it is still possible to write the aeroelastic equations in a state-space form [20, 33, 34]. The approach adopted here may then still be

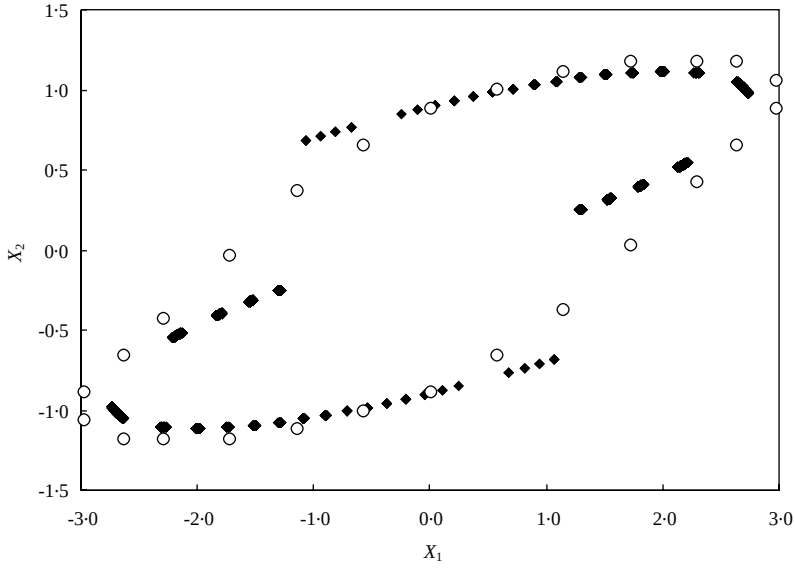

Figure 16. Domain of attraction for System II, $V = 1{\cdot}0903286$, initial conditions: $\dot{X}_1^{(0)} = 0{\cdot}0$, $\dot{X}_2^{(0)} = 0{\cdot}0$; ○, time domain prediction; ◆, stable manifold analysis.

TABLE 2

Values of λ_1, λ_2, ω_1, and ω_2 for the averaged form of equations for System II

V	λ_1	λ_2	ω_1	ω_2	$\omega_1 - \omega_2$
1·000167	0·0004571	− 0·0174105	1·006550	1·012990	− 0·006440
1·006457	0·0118610	− 0·0288395	1·008440	1·011240	− 0·002800
1·090329	0·0620660	− 0·0790194	1·010430	1·011150	− 0·000720

applicable. Indeed, centre manifold analysis has successfully been applied to such an aeroelastic system [20].

REFERENCES

1. S. F. SHEN 1959 *Journal of the Aeronautical Sciences* **28**, 25–32, 45. An approximate analysis of certain non-linear flutter problems.
2. E. BREITBACH 1978 *AGARD-R-665*. Effects of structural non-linearities on aircraft vibration and flutter.
3. E. BREITBACH 1980 *NASA TP* 1620. Flutter analysis of an airplane with multiple structural non-linearities in the control system.
4. R. M. LAURENSON and R. M. TRN 1980 *American Institute of Aeronautics and Astronautics Journal* **18**, 1245–1251. Flutter analysis of a missile control surface containing structural non-linearities.
5. R. P. BRILEY and J. L. GUBSER 1982 *McDonnell Douglas Astronautics Company, St. Louis, Final Report* (*Contract F*49620-82-*C*-0043). Investigation of limit cycle response of aerodynamic surfaces with structural non-linearities.
6. C. L. LEE 1984 *Ph.D. Dissertation, Southern Methodist University, Dallas, Texas*. Aeroelastic stability analysis with interacting structural non-linearities.

7. R. M. LAURENSON, A. J. HAUENSTEIN, and J. L. GUBSER 1986 *AIAA Paper* 86-0899. Effects of structural non-linearities on limit cycle response of aerodynamic surfaces.
8. C. L. LEE 1986 *American Institute of Aeronautics and Astronautics Journal* **24**, 833–839. An iterative procedure for non-linear flutter analysis.
9. A. P. LEWIS 1994 *Aerospace Vehicle Dynamics and Control*. Oxford: Clarendon Press. The aeroelastic behaviour of a missile control fin with a pneumatic actuation system.
10. L. MORINO 1969 *American Institute of Aeronautics and Astronautics Journal* **7**, 405–411. A perturbation method for treating non-linear panel flutter problems.
11. E. H. DOWELL 1984 *Transactions of the American Society of Mechanical Engineers, Journal of Applied Mechanics* **51**, 664–673. Observation and evolution of chaos for an autonomous system.
12. R. R. REYNOLDS and E. H. DOWELL 1993 34*th AIAA/ASME/ASCE/AHS/ASC Structures, Structural Dynamics and Materials Conference, ISSN* 0161-5750, 2566–2576. Non-linear aeroelastic response of panels.
13. T. V. SMETLOVA and E. H. DOWELL 1994 *American Society of Mechanical Engineers, Applied Mechanics Division, AMD* **192**, 327–332. On necessary conditions for chaotic motion of a buckled plate with external excitation in an aerodynamic flow.
14. D. TANG, D. KHOLODAR and E. H. DOWELL 2000 41*st AIAA/ASME/ASCE/AHS/ASC Structures, Structural Dynamics and Materials Conference, ISSN* 0273-4508, **1**, 1514–1523. Non-linear aeroelastic response of a typical airfoil section with control surface freeplay.
15. S. T. TRICKEY, L. N. VIRGIN and E. H. DOWELL 2000 41*st AIAA/ASME/ASCE/AHS/ASC Structures, Structural Dynamics and Materials Conference, ISSN* 0273-4508 Vol. **1**, 57–62. Characterizing stability of responses in a non-linear aeroelastic system.
16. D. TANG, D. KHOLODAR and E. H. DOWELL 2000 *American Institute of Aeronautics and Astronautics Journal* **38**, 1543–1557. Non-linear response of an airfoil section with control surface freeplay to gust loads.
17. P. J. HOLMES and D. A. RAND 1975 *Technical Report No.* 79, *University of Southampton Institute of Sound and Vibration Research*. Identification of vibrating systems by generic modelling, with an application to flutter.
18. J. ANDERSON 1995 *International Forum on Aeroelasticity and Structural Dynamics, Royal Aeronautical Society, ISBN* 1 85768 086 3, 84·1–84·11. Conjectures on new transonic aeroelastic phenomena.
19. J. GRZEDZINSKI 1995 *International Forum on Aeroelasticity and Structural Dynamics, Royal Aeronautical Society, ISBN* 1 85768 086 3, 61·1–61·11. Flutter calculation on an aircraft with non-linear structure based on center-manifold reduction.
20. L. LIU, Y. S. WONG and B. H. K. LEE 2000 *Journal of Sound and Vibration* **234**, 641–659. Application of the centre manifold theory in non-linear aeroelasticity.
21. A. SEDAGHAT, J. E. COOPER, J. R. WRIGHT and A. Y. T. LEUNG 2000 41*st AIAA/ASME/ASCE/AHS/ASC Structures, Structural Dynamics and Materials Conference, ISSN* 0273-4508, **1**, 499–507. Limit cycle oscillation prediction for aeroelastic systems with continuous non-linearities.
22. D. E. GILSINN 1975 *SIAM Journal on Applied Mathematics* **29**, 628–660. The method of averaging and domains of stability for integral manifolds.
23. H. CHIANG, M. W. HIRSCH and F. F. WU 1988 *IEEE Transactions on Automatic Control* **33**, 16–27. Stability regions of nonlinear autonomous dynamical systems.
24. V. VENKATASUBRAMANIAN and W. JI 1997 *Automatica* **10**, 1877–1883. Numerical approximation of $(n-1)$-dimensional stable manifolds in large systems such as power systems.
25. H. ASHLEY and G. ZARTARIAN 1956 *Journal of the Aeronautical Sciences* **23**, 1109–1118. Piston theory—a new aerodynamic tool for the aeroelastician.
26. N. MINORSKY 1962 *Non-Linear Oscillations*. Princeton, NJ: D. Van Nostrand Company, Inc.
27. I. N. HAJJ and S. SKELBOE 1980 *Proceedings—IEEE International Symposium on Circuits and Systems*, **3**, 905–908. Solution trajectories in piecewise-linear dynamic systems.
28. K. OKUMURA and A. KISHIMA 1983 *Electronics and Communications in Japan* **66**, 1–10. Numerical technique of perturbation method for computing periodic solution of piecewise-linear autonomous system.
29. R. J. KAYE and A. SANGIOVANNI-VINCENTELLI 1983 *IEEE Transactions on Systems, Man and Cynernetics* **13**, 465–469. Solution of piecewise-linear ordinary differential equations using waveform relaxation and Laplace transforms.

30. H. IMAMURA and K. SUZUKI 1991 *Transactions of the Japan Society of Mechanical Engineers* **57**, 2811–2818. Global representation of general solution and canonical forms for piecewise linear oscillators (the case of a discontinuous non-linearity).
31. C. W. WONG, W. S. ZHANG and S. L. LAU 1991 *Journal of Sound and Vibration* **149**, 91–105. Periodic forced vibration of unsymmetrical piecewise-linear systems by incremental harmonic balance method.
32. E. CHICUREL-UZIEL 2001 *Journal of Sound and Vibration* **245**, 285–301. Exact single equation, closed-form solution of vibrating systems with piecewise linear springs.
33. J. LEISHMAN and G. CROUSE 1989 *AIAA Paper* 89-0022. A state-space model of unsteady aerodynamics in a compressible flow for flutter analyses.
34. W. LIN and W. CHENG 1993 *Journal of the Chinese Society of Mechanical Engineers* **14**, 456–466. Nonlinear flutter of loaded lifting surface (II).

APPENDIX A: NUMERICAL DATA FOR AEROELASTIC MODELS

The lifting surface considered in these studies had the geometric characteristics shown in Figure A1. Thickness effects are neglected.

The mode shapes, together with generalized mass and stiffness data are given in Tables A1 and A2.

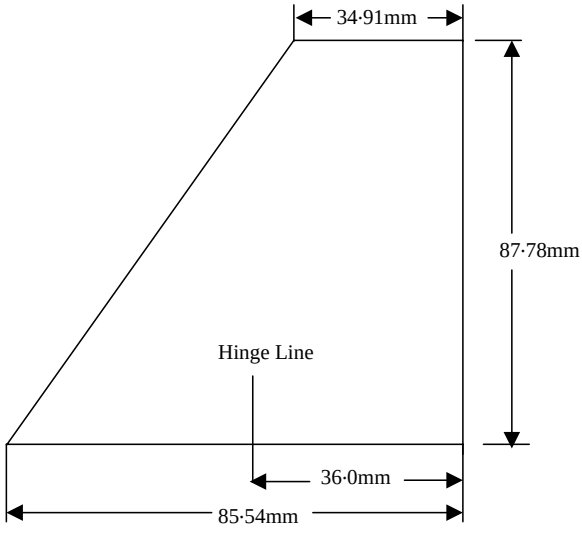

Figure A1. Lifting surface geometry.

TABLE A1

Modal data

Strip Number s	$2b_s$ (mm)	$2b_s x_{os}$ (mm)	ϕ^F_{1s}	ϕ^F_{2s}	ψ^F_{1ys}	ψ^F_{2ys}
1	80·4738	46·6290	$-2{\cdot}125213\times10^{-3}$	$3{\cdot}124895\times10^{-3}$	1·000000	1·158449
2	70·3494	40·7550	$-6{\cdot}375600\times10^{-3}$	$1{\cdot}528817\times10^{-2}$	1·000000	1·133542
3	60·2250	34·8810	$-1{\cdot}062600\times10^{-2}$	$3{\cdot}386578\times10^{-2}$	1·000000	1·078578
4	50·1006	29·0070	$-1{\cdot}487640\times10^{-2}$	$5{\cdot}785579\times10^{-2}$	1·000000	1·041359
5	39·9762	23·1330	$-1{\cdot}912680\times10^{-2}$	$8{\cdot}590975\times10^{-2}$	1·000000	1·005500

TABLE A2

Generalized mass and stiffness data

Mode Number i	a_i^F	e_i^F	ψ_{iy0}^F
1	$5{\cdot}562880 \times 10^{-5}$	0·0	1·000000
2	$3{\cdot}477841 \times 10^{-4}$	$1{\cdot}589684 \times 10^{3}$	1·184876

APPENDIX B: NOMENCLATURE

$\mathbf{A}$	Jacobian defining linear terms of averaged equations (31)
$\mathbf{A}_s$	Jacobian of equations for stable dynamics of averaged system
a_1, a_2, a_3, a_4	Slowly varying variables in averaging procedure
A_1, A_2	Amplitudes of a_1, a_2, a_3, a_4
a_i^F	ith generalized mass of control surface
a_∞	Free stream speed of sound
b	Control surface root semi-chord
b_s	Mean semi-chord for sth strip of control surface
e_i^F	ith generalized stiffness of control surface
d_{ij}^F	Structural damping coefficient
$\mathbf{G}_2$	Matrix defining second order terms of $R_u(u_1, u_2, 0)$
$\mathbf{G}_{3u}$	Matrix defining third order terms of $R_u(u_1, u_2, h_2)$
$\mathbf{G}_{4u}$	Matrix defining fourth order terms of $R_u(u_1, u_2, h_2 + h_3)$
$\mathbf{G}$	Damping matrix in aeroelastic equations
$\mathbf{H}$	Stiffness matrix in aeroelastic equations
$\mathbf{H}_2, \mathbf{H}_3, \mathbf{H}_4$	Matrices defining second, third and fourth order terms of stable manifold
h	Function defining stable manifold
h_2, h_3, h_4	Functions defining second, third and fourth order terms of stable manifold
h_s	Vertical displacement of sth strip at point O_s
I_{ij}	Coefficient of $\dot{X}_j$ in equation for generalized aerodynamic force Q_{Ai}
$I_{1s}, \ldots, I_{5s}$	Integrals depending on control surface thickness used in aerodynamics
K	Linear torsional stiffness at root
L_s	Load per unit span for sth strip
$\mathbf{K}_1, \mathbf{K}_2$	Matrices defining second order terms of $\mathbf{R}_s(u_1, u_2, 0)$
$\mathbf{L}_1, \mathbf{L}_2$	Matrices defining third order terms of $\mathbf{R}_s(u_1, u_2, h_2)$
$\bar{\mathbf{M}}$	Right-hand modal matrix in solution of linearized aeroelastic equations
$\bar{\mathbf{N}}$	Left-hand modal matrix in solution of linearized aeroelastic equations
M_∞	Free stream Mach number
M_s	Torsional moment per unit span for sth strip about O_s
Q_1, Q_2, Q_3, Q_4	Generalized co-ordinates arising from transforming $\mathbf{X}$ and $\mathbf{Y}$
Q_{Ai}	ith generalized aerodynamic force
Q_{Mi}	ith generalized force on fin due to torsional reaction loads
R_{ij}	Coefficient of X_j in equation for generalized aerodynamic force Q_{Ai}
$\mathbf{R}$	Non-linear terms of averaged system of equations
$\mathbf{R}_s$	Non-linear terms of equations for stable dynamics of averaged system
R_u	Non-linear terms of equation for unstable dynamics of averaged system
$\mathbf{r}$	Column vector relating fin root torsion angle to generalized displacements in aeroelastic equations
$\mathbf{s}$	Column vector used in defining non-linear terms in aeroelastic equations
t	Time
t'	Non-dimensionalized time ($= \tilde{\omega}t$)
U_∞	Free stream velocity
u_1, u_2	Independent variables in equation for stable manifold
V	Non-dimensionalized speed in aeroelastic equations
x_s, y_s, z_s	Co-ordinates for sth strip

x_{os}	Non-dimensional distance of O_s from leading edge of sth strip
X_1, X_2	Generalized displacements
$\mathbf{X}$	Column vector of generalized displacements
$\mathbf{Y}$	Derivative of $\mathbf{X}$ with respect to time
w	Downwash on control surface
γ	Ratio of specific heats
δ	Freeplay parameter
Δh	Strip width
ε	Non-linearity parameter
θ_s	Pitch rotation of sth strip
θ_y	Pitch rotation of control surface at root
ρ_∞	Free stream density
$\tau_s(x_s)$	Non-dimensional thickness distribution function for sth strip
ϕ_i^F	ith natural mode for control surface
ϕ_{is}^F	ith modal displacement of the sth strip
ψ_{iys}^F	ith modal pitch rotation of the sth strip
ψ_{iy0}^F	ith modal pitch rotation of control surface at root
$\tilde{\omega}$	Frequency used in non-dimensionalizing time t
ω_i^F	ith natural frequency of control surface
ω_1, ω_2	Frequencies in solution of linear aeroelastic system